# SIZE AND DENSITY-DEPENDENT SURVIVAL IN A BROWN SHRIMP (*Farfantepenaeus aztecus*) POPULATION

A Thesis

by

CYRENEA BRAGDON PIPER

Submitted to the Office of Graduate and Professional Studies of
Texas A&M University
in partial fulfillment of the requirements for the degree of

MASTER OF SCIENCE

| | |
|---|---|
| Chair of Committee, | Masami Fujiwara |
| Committee Members, | Kirk O Winemiller |
| | Hui Liu |
| Head of Department, | Michael Masser |

December 2017

Major Subject: Wildlife and Fisheries Sciences

# ABSTRACT

Compensatory density dependence is required for sustainable harvest of any stock and is assumed in brown shrimp stock assessments. However, the strength and mechanisms of this density dependence and the developmental stage upon which it acts on has not been identified for this species. In general, detecting density dependence is complicated by the need for data at the appropriate temporal and spatial scales and the presence of environmental variability, observation error and other process error. Previous research indicated that compensatory processes might affect the juvenile stage of brown shrimp. Using Bayesian methods, I fitted state space matrix population models to 11 years of length-specific count data of juvenile brown shrimp sampled a maximum of eight times per month in Caranchua Cove Galveston Bay, Texas. I evaluated the influence of size-dependent survival, Beverton-Holt density-dependent survival and size-dependent growth on the juvenile stage. Using information criteria to evaluate model fit, I found that size-dependent survival was the most important factor acting on this population, followed by density-dependent survival. To avoid over-parameterization of the model, I omitted environmental factors such as temperature and salinity, that have a strong influence on juvenile brown shrimp growth and survival. As a result, models had poor fit and low predictive value; consequently, parameter estimates should be viewed with caution. Due to convergence issues, I was unable to test both size and density-dependent survival in a single model. The presence of density-dependent survival in the juvenile stage of this population suggests that this is the regulating stage in the brown shrimp lifecycle. This study provides a first step in identifying the stage and mechanisms regulating brown shrimp populations to better inform management.

# ACKNOWLEDGMENTS

I would like to thank my committee chair, Dr. Fujiwara of the Department of Wildlife and Fisheries Sciences at Texas A&M University for his unfailing support, for providing me invaluable guidance throughout this process and for his patience while I pursued a full-time career while completing this thesis. I would like to thank my committee members, Dr. Winemiller and Dr. Liu, and Dr. Minello for their support and guidance through the course of this research. I would also like to thank Dr. Can Nioc for his invaluable assistance with my analyses and his willingness to help me learn Bayesian statistics.

Finally, I must express my profound gratitude to my husband and my mother for their patience and support throughout the process of researching and writing this thesis. This accomplishment would not have been possible without them. Thank you.

# CONTRIBUTORS AND FUNDING SOURCES

## Contributors

This work was supervised by a thesis committee consisting of Dr. Masami Fujiwara (advisor) and Dr. Kirk O. Winemiller of the Department of Wildlife and Fisheries Sciences and Dr. Hui Liu of the Department of Marine Biology.

The data analyzed was provided by Dr. Tom Minello of National Oceanic and Atmospheric Administration Fishery Ecology Branch, Galveston Bay, Texas. The analyses conducted for this thesis were conducted with the assistance of Dr. Can Nioc, currently a post-doctoral researcher at Virginia Tech. All other work conducted for the thesis was completed by the student independently.

## Funding Sources

Graduate study was supported in part by an Excellence Fellowship from Texas A&M University, and an Institutional Grant (NA10OAR4170099) to the Texas Sea Grant College Program from the National Sea Grant Office, National Oceanic and Atmospheric Administration, U.S. Department of Commerce.

# TABLE OF CONTENTS

# LIST OF FIGURES

Page

# LIST OF TABLES

Page

# 1. INTRODUCTION

The Gulf of Mexico shrimp fishery is one of the most important fisheries in the United States, with commercial brown shrimp fisheries contributing an average of 105 million pounds of brown shrimp to the U.S. fish market annually, valued at an average $182 million in yearly landings revenue between 1995 and 2015 (NOAA Fisheries Statistics 2015. ; Voorhees 2011). The economic contribution of brown shrimp makes accurate harvest predictions an economic priority (Baxter and Sullivan 1986; Voorhees 2011) and quantifying the compensatory processes acting on brown shrimp is critical to these harvest predictions (Nance 1989; Rose et al. 2001).

Sustainable harvest depends on the assumption of compensatory density dependence, the ability of a population to increase recruitment rate, growth rate, and/or survival rate to counteract an increased mortality rate from harvesting (Anderson 1988; Rose et al. 2001; Sinclair and Pech 1996; Sissenwine 1984). The magnitude of compensation, however, is a principal source of uncertainty in fisheries management (Fogarty et al. 1991; Rose et al. 2001). Very strong compensatory processes can obscure the relationship between adult stock and juvenile recruitment (Fogarty et al. 1991; Shepherd et al. 1990; Sissenwine 1984), which can lead managers to assume compensation without direct evidence. Brown shrimp stock assessments, for example, assumed a Beverton-Holt stock-recruit relationship to explain the resilience of brown shrimp stock under exploitation even though there was no statistically discernible stock-recruitment relationship (Hart 2012; Nance 1989; Nance 2008; Nichols 1984). This assumption has led to the conclusion that overfishing of brown shrimp is nearly impossible (Lassuy 1983), a type of conclusion that can put exploited fish populations at risk (Hilborn and Walters 2013; Rose et al. 2001), especially if sea level rise and the resulting loss of marsh habitat leads to declining productivity and recruitment (Nance 1989; Scavia et al. 2002).

Determining how a population will respond to exploitation requires determining the relative importance of density-independent and density-dependent processes on recruitment (Fogarty et al. 1991). Environmental variability, however, can obscure evidence of compensatory processes making detection and extrapolation of the mechanisms driving compensation difficult (Fogarty et al. 1991; Sissenwine 1984). Brown shrimp production in the Gulf of Mexico, for example, is highly variable from year to year (NOAA Fisheries Statistics 2015) and highly dependent on environmental conditions (Nance 1989; Nance 2014; Nance 2015; Nance 2016), which would be expected to make detection of density

dependence difficult (Anderson 1988; Fogarty et al. 1991; Houde 1997; Shepherd et al. 1990; Sissenwine 1984). Compensation, however, must exist in all populations at some stage or the population would eventually go extinct (Murdoch 1994). The question, therefore, is not whether compensation exists in a population, but rather, what is the strength of compensation and on which developmental stages does compensation act? To answer these questions, we must first understand the main compensatory mechanisms acting on the population (Murdoch 1994; Rose et al. 2001).

The objective of this study was to improve our understanding of the main compensatory mechanisms acting on juvenile brown shrimp. More specifically, these analyses were conducted to determine if survival and/or growth of juvenile brown shrimp in Carancahua Cove at Galveston Bay Texas were regulated by Beverton-Holt density dependence, size dependence, both, or neither by identifying the main ecological processes acting on juvenile brown shrimp in estuaries and incorporating these processes into competing population models.

### 1.1 Harvest Forecasting

The juvenile stage of brown shrimp has been the best predictor of recruitment to and abundance in the adult stage (Baxter and Sullivan 1986; Haas et al. 2001; Sogard 1997). Eggs and larvae of marine fish are subject to high mortality rates and are, therefore, poor predictors of recruitment and cohort strength (Houde 1987; Houde 1989; Pepin 1991). This may, in brown shrimp, be because physical dispersal to suitable areas and food availability is independent of density or size of individuals (Anderson 1988; Cushing 1990; Hjort 1914; Sogard 1997). Post-larval brown shrimp abundance, the stage at which shrimp enter estuaries, is the earliest stage that correlates with recruitment. It is, however, the least accurate and is not described well by any model (Baxter and Sullivan 1986; Haas et al. 2001). Sub-adult (bait-size) shrimp abundance is a more accurate predictor of adult brown shrimp abundance, but it is the least timely, giving managers very little time between sampling and determining harvest quotas (Baxter and Sullivan 1986). Juvenile abundance is a more precise predictor of adult abundance than the post larval stage and provides more timely information than the bait-size shrimp stage (Baxter and Sullivan 1986).

Current brown shrimp harvest forecasts include juvenile and subadult abundance combined with salinity, temperature and tidal height, a measure of marsh accessibility. In recent years, brown shrimp harvest forecasts have been below historical averages as a result of extreme environmental conditions (Nance 2014; Nance 2015; Nance 2016). These recent forecasts highlight the importance of quantifying the influence of both environmental conditions and density dependence on brown shrimp recruitment,

especially as environmental conditions and habitat quality and quantity become more variable with global climate change (Scavia et al. 2002). By identifying the presence and mechanisms of density dependence, this study will improve brown shrimp recruitment and harvest predictions and improve managers' understanding of how changing environmental factors may affect shrimp populations in the future (Haas et al. 2001).

### 1.2 Study Species

Brown shrimp in the Gulf of Mexico have an annual life cycle whereby adults spawn in open water throughout the year, producing planktonic larvae that migrate as postlarvae and settle in estuaries (Lassuy 1983). Spawning peaks between September and November and between April and May (Baxter and Renfro 1967; Cook and Lindner 1970; Lassuy 1983). Settlement occurs when shrimp are 8-15 mm in body length during flood tides throughout much of the year, peaking in the spring and the fall, spring peak settlement occurs between February and June, and fall peak settlement occurs between August and September; however, there is some disagreement over when peak settlement occurs and whether there is a fall peak (Baxter and Renfro 1967; Lassuy 1983; Nance 1989; Wenner and Beatty 1993).

Juveniles remain in shallow estuarine habitat for approximately three months (Lassuy 1983), during which temperature (Anderson 1988; Haas et al. 2001; Sissenwine 1984), salinity (Rozas and Minello 2011; Zimmerman et al. 1991), and access to submerged marsh and marsh edge are thought to be the most important environmental factors affecting brown shrimp survival and growth (Childers et al. 1990; Roth et al. 2008; Zimmerman et al. 1984). Upon reaching 60 – 70 mm, subadult shrimp recruit from shallow nursery habitats to open bay staging areas before moving to offshore spawning grounds when they are 77 – 110 mm (Knudsen et al. 1985; Lassuy 1983). Adult brown shrimp are less subject to predation in coastal waters than juveniles and subadults in estuaries, but are subject to fishing mortality between May and September (Divita et al. 1983; Lassuy 1983; Minello et al. 1989; Nance 1989).

### 1.3 Environmental Factors

Growth and survival of juvenile brown shrimp are affected by metabolic requirements. Temperature (Anderson 1988; Haas et al. 2001; Sissenwine 1984) and salinity alter metabolic costs, affecting growth and survival of brown shrimp (Clark et al. 2004; Doerr et al. 2016; Rozas and Minello 2011; Rozas and Reed 1994; Saoud and Davis 2003). These environmental processes have strong effects on shrimp, independent of shrimp size and population densities, but were not explicitly included in this analysis, rather they were included in the process error parameter (see 2.2 Error).

Brown shrimp size is directly related to growth and survival throughout their development. With increasing size, brown shrimp more successfully exploit prey resources and are subject to lower rates of predation, a major source of juvenile mortality (Anderson 1988; Divita et al. 1983; Minello et al. 1989; Nance 1989; Ware 1975; Werner and Gilliam 1984). Because size and mortality are strongly linked in fish (Sogard 1997; Ware 1975; Werner and Gilliam 1984) and in brown shrimp (Minello et al. 1989), I expect size-dependent mortality during the juvenile stage to be a strong force acting on this brown shrimp population.

Brown shrimp select *Spartina alterniflora* marsh over nonvegetated habitat (Minello et al. 2008; Zimmerman and Minello 1984; Zimmerman et al. 1984) and marsh edge over inner marsh (Minello and Webb Jr 1997; Minello et al. 2008; Minello and Rozas 2002; Minello and Zimmerman 1991; Minello et al. 1989; Minello et al. 1994; Rozas et al. 2007; Rozas and Zimmerman 2000; Whaley and Minello 2002). Access to vegetated marsh edge provides refuge from predation (Boesch and Turner 1984; Kneib 1995; Minello and Wooten Jr 1993; Minello and Zimmerman 1991; Minello et al. 1989; Roth et al. 2008), decreases the risk of stranding with ebbing tides by providing access to productive marsh habitat while allowing for quick escape when tides retreat (Kneib and Wagner 1994; Kneib 1984; Minello et al. 2012), and provides greater access to infaunal prey (Rozas and Zimmerman 2000; Whaley 1997). These, in turn, can lead to increased brown shrimp growth (Cowan Jr et al. 1997; McTigue and Zimmerman 1998; Minello and Zimmerman 1991; Rozas and Odum 1988) and survival (Childers et al. 1990; Roth et al. 2008; Zimmerman and Minello 1984).

Access to vegetated marsh edge can depend on brown shrimp densities. As brown shrimp densities increase, available vegetated marsh edge per individual decreases, resulting in contest competition. Consequently, some brown shrimp have access to refuge and prey resources, while others are forced to use less beneficial habitat, resulting in higher risk of predation (Kneib 1995; Minello and Zimmerman 1983; Minello et al. 1989) and less access to prey (McTigue and Zimmerman 1998; Rozas and Zimmerman 2000). Because juvenile brown shrimp are subject to higher stranding probability with ebbing tides, higher predation rates and less availability of prey away from vegetated marsh edge, I hypothesize that competition for vegetated marsh edge results in density-dependent survival and growth in the estuarine-dependent juvenile stage.

# 2. METHODS

Detection of density dependence is limited by the presence of observation error and process error in the data (Freckleton et al. 2006; Knape and de Valpine 2012); mismatch between the temporal (Anderson 1988) and spatial scales of the data (Houde 1989; May 1986; Ray and Hastings 1996); and the need for enough variation in the data to capture the compensatory response of a population (May 1986; Murray 1994; Rose et al. 2001). I applied a Bayesian state-space method, using monthly averages of length-specific density estimates collected over 11 years in Galveston Bay, Texas to test for size-dependent and density-dependent survival and size-dependent growth in juvenile brown shrimp (*Farfantepenaeus aztecus*). This length-specific time series provides a rare opportunity to examine fine scale temporal processes affecting survival and growth of juvenile brown shrimp. Using a stage-structured matrix population model for a part of the lifecycle, I tested for size- and density-dependent regulation of juveniles, incorporating survival, growth, and settlement in a state-space framework, which separates observation and process error, to estimate the demographic parameters. I used the Beverton-Holt survival model (see "Density-Dependent Survival Models" in "Methods") to represent contest competition (Brännström and Sumpter 2005; Sissenwine 1984), whereby a fixed quantity of habitat is available and some individuals have what they need to grow and survive, while others do not (Hassell 1975). Because size-dependent growth and mortality are linked, I incorporated size-dependent survival and size-dependent growth in the juvenile stage (Anderson 1988; Pauly 1980). I used deviance information criteria (DIC) (Spiegelhalter et al. 2002) to compare the NULL model (size- and density-independent model) and four alternative models: size-dependent growth, size-dependent survival, within stage density-dependent survival and between stage density-dependent survival.

## 2.1 Data

Juvenile Brown shrimp data were collected by the National Marine Fisheries Service in Carancahua Cove at Galveston Bay, Texas. These data were collected during the day from two types of habitat, *Spartina alterniflora* marsh edge (SAME) and shallow nonvegetated bottom (SNB) (Rozas et al. 2007) using a 1.8m drop sampler (Zimmerman and Minello 1984) when both habitat types were submerged but less than 1m deep. Samples were taken during the day between March 1982 and December 1992. Sampling was attempted 8 times per month per habitat type. However, due to low water levels, sampling was not always possible. The number and size of individuals caught were recorded as paired samples by habitat type. For these analyses, data paired by habitat type were combined because shrimp move between

habitats within one time step (30 days). Length-specific counts were converted to density estimates with a conversion factor used to adjust for the total area of SAME or SNB in 1 hectare of Carancahua Cove (see Figure 1). This conversion factor was adjusted based on changes in total area of SAME and SNB in Carancahua Cove based on aerial surveys over the study period and Geographic Information System analyses (Rozas et al. 2007).

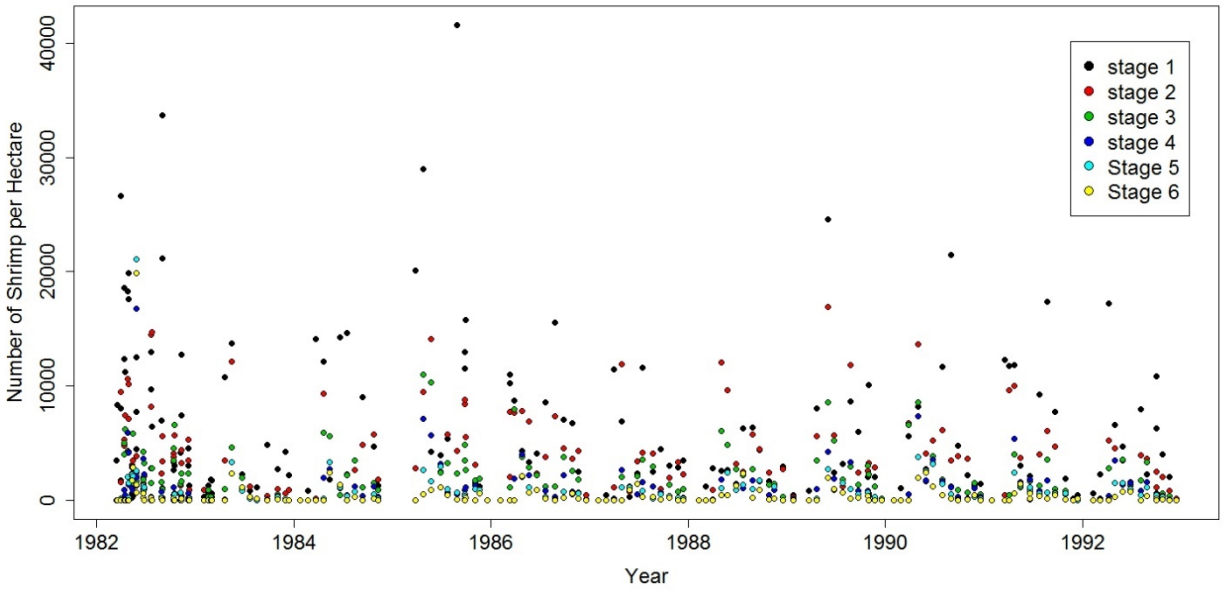


Figure 1: Stage specific number of shrimp per hectare between 1982 and 1992 in Caranchua Cove at Galveston Bay, Texas.

The sampling period in this study captures 11 years and considerable variation in marsh area and edge length over the sampling period, with much of the habitat transitioning from wetlands to shallow open water during the study (Rozas et al. 2007), which I expect led to a compensatory response in the data. The length of this time series, which include both high and low population densities where density-dependent effects can be strongly contrasted, is expected to make detection of density dependence more likely (Brook and Bradshaw 2006; Hixon 1998; Knape and de Valpine 2012; May 1986; Murray 1994; Rose et al. 2001; Sissenwine 1984; Turchin 1999).

### 2.2 Error

There are four main sources of error: process variance, observation variance, variation among individuals, and uncertainty in model selection (Hobbs and Hooten 2015). Models must account for these errors for unbiased detection of density dependence (Freckleton et al. 2006; Knape and de Valpine 2012). Process error results from the inability to represent all processes that cause variation in population density within a model. Process error includes, among other things, density-independent environmental factors, such as temperature and salinity, known to affect shrimp survival and growth, as well as demographic stochasticity. To avoid overparamaterization of the models, these environmental factors could not be included in the models explicitly. Instead, they were included in one term, which I call process error. Observation error results from an inability to take an infinite number of samples and the inherent errors that result from sampling a population; consequently, samples are not a perfect representation of true population densities (Hobbs and Hooten 2015).

If process and observation errors are not separated, one may erroneously detect density dependence when it is not present (Dennis et al. 2006; Freckleton et al. 2006). To improve the chance of accurately detecting density dependence in this population and to reduce the chance of biased estimates of density dependence, I used the state-space method to separately account for process and observation errors (de Valpine and Hastings 2002; Lebreton and Gimenez 2013). I accounted for variation among individuals by letting growth and survival vary with stage in some models. Finally, to account for model uncertainty, I fit multiple models and selected the best model using DIC (Hobbs and Hooten 2015; Spiegelhalter et al. 2002).

### 2.3 The Stage-Based Matrix Model

The stage-based matrix model consists of six stages categorized by body length in 10 mm increments. Stage 1 includes individuals 10-20 mm, stage 2 includes individuals 21-30 mm, and so on until they reach the final stage included in the model, stage 6, which includes individuals 61-70 mm. Individuals first survive ($\varphi_i$), where $\varphi_i$ is the proportion of individuals in stage i surviving over one time step (30 days). The time step of my analyses was limited to a minimum of 30 days by the data, because some samples were taken irregularly within a given month. Next, individuals transition ($\gamma_{ji}$), where $\gamma_{ji}$ is the proportion of individuals transitioning from stage i to stage j, and a transition is the probability that an individual grows 20-30, 31-40, or 41 or more mm per time step (30 days) (see Figure 2). Cook and Lindner (1970) summarized past growth rates, which ranged from 1.0-2.5 mm/day and Haas et al. (2004) assumed an average growth rate of 1mm/day in a brown shrimp model. Accordingly, I assumed a minimum growth

rate of 20 mm per time step or that individual does not survive. Seasonal settlement in the marsh is defined by $c_{is}$, the proportion of individuals that settle in stage "i" in season "s" (see Table 1).

Table 1: Seasonal shrimp settlement ($c_{is}$).

| Season (*s*) | Months |
|---|---|
| 1 | December, January, February |
| 2 | March, April, May |
| 3 | June, July, August |
| 4 | September, October, November |

The input of individuals into stages 1 and 2 is a function of seasonal settlement only. The number of individuals in stage 3 is a function of settlement, growth from stage 1, survival in stage 3, and growth to larger stages. The number of individuals in stages 4 - 6 is a function of survival and growth, but there is no settlement. I assume individuals recruit offshore (i.e. emigration) at 70 mm or longer (Knudsen et al. 1985; Lassuy 1983), consequently, survival and growth may be confounded with individuals recruiting offshore in all but stage 1 (Figure 2). The effects of density-dependent and size-dependent factors on survival and growth are assumed to occur within a single time step, and individuals are assumed to be homogeneous within a given stage, with the same probability of growth and survival. Finally, I assume an annual model with 12 seasons and a single shrimp population.

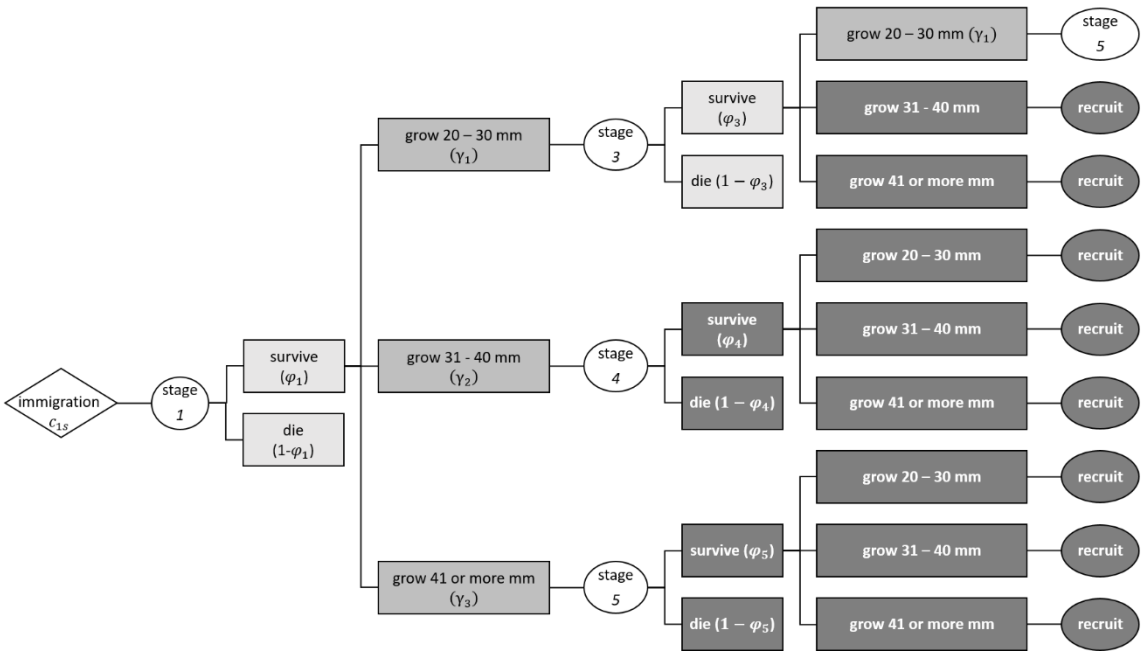


Figure 2: Diagram showing the progression of an individual through life stages where an individual immigrates ($c_{is}$) into stage 'i' in season 's,' the individual in stage 'i' either survives ($\varphi_i$) or dies (1-$\varphi_i$). If the individual survives, it must grow either 20-30 mm ($\gamma_{(i+2)i}$), 31-40 mm ($\gamma_{(i+3)i}$,) or 41 mm or more ($\gamma_{(i+4)i}$) to transition to the next stage. Diamonds indicate immigration, circles indicate stage, rectangles with light grey indicate survival or death, rectangles with medium grey indicate transitions between stages via growth, rectangles with dark grey and white text indicate parameters not estimable because they are confounded with emigration.

### 2.4 The State Space Model

The state-space model consists of two submodels: the observation model (1) and the process model (2) (Harvey 1990).

$$\mathbf{y}_{\mathrm{i,time=t+1}} = \mathbf{x}_{\mathrm{i,time=t+1}} + \boldsymbol{\varepsilon}_{\mathrm{time=t}} \quad (1)$$

$$\mathbf{x}_{\mathrm{i,time=t+1}} = \mathbf{AZx}_{\mathrm{i,time=t}} + \mathbf{c}_{\boldsymbol{stage=i,season=s}} + \boldsymbol{\omega}_{\mathrm{time=t}} \quad (2)$$

Where vector $\boldsymbol{y}$ $(6 \times 1)$ represents the observed density in each size class at time $\mathrm{t}+1$ on the natural log scale, vector $\boldsymbol{x}$ $(6 \times 1)$ represents the corresponding true density on the natural log scale. The elements of matrix **A** represents the growth processes, matrix **Z** represents survival and density-dependent processes, which are implemented differently for different sub-models, vector $\boldsymbol{c_{is}}$ is the seasonal settlement and $\boldsymbol{\omega}_{\mathrm{t}}$ and $\boldsymbol{\varepsilon}_{\mathrm{t}}$ are vectors of process and observational errors. It is assumed that each size class has independent and identical normal process and observational errors. Vector $\boldsymbol{c_{is}}$ $(6 \times 1)$ where $c_{is} = [c_{1s}, c_{2s}, c_{3s}, 0, 0, 0]^T$ represents settlement level at stage $i$ season $s$. It is assumed that settlement levels only change among different seasons.

In the process model (1), the latent state variable denoted by $\mathbf{x}_{i,t+1}$ is the natural log of the true density of stage i at time $t+1$ and is a function of $\mathbf{x}_{i,t}$, the vector of densities for stage i at time $t$ and the processes describing the transition from one stage to the next. These processes are survival (**Z**), growth (**A**), and immigration (**c**), with process error $\omega_t$. Matrix **Z** $(6 \times 6)$ represents survival rates where $\varphi_i$ is the probability an individual in stage i survives. Matrix **A** $(6 \times 6)$ represents individual growth rates where $\gamma_{ji}$ is the probability an individual grows and subsequently transitions from stage i to stage j.

Process error $(\omega_t)$ accounts for environmental and demographic stochasticity and is assumed to be normal with a zero mean and variance $\sigma^2$.

The state variable $\mathbf{y}_{i,t+1}$ represents the observed population density of stage i at time $t+1$, which is a function of the latent state variable $(\mathbf{x}_{i,t+1})$ and the observation error $(\varepsilon_t)$. Observation error $(\varepsilon_t)$ accounts for "sampling effect" and is assumed to be normal with a zero mean and variance $\tau^2$ (Clark and Bjørnstad 2004). See Figure 3 for a graphical representation of the relationship between these variables.

$$\boldsymbol{Z} = \begin{bmatrix} \varphi_1 & 0 & 0 & 0 & 0 & 0 \\ 0 & \varphi_2 & 0 & 0 & 0 & 0 \\ 0 & 0 & \varphi_3 & 0 & 0 & 0 \\ 0 & 0 & 0 & \varphi_4 & 0 & 0 \\ 0 & 0 & 0 & 0 & 0 & 0 \\ 0 & 0 & 0 & 0 & 0 & 0 \end{bmatrix}$$

$$\boldsymbol{A} = \begin{bmatrix} 0 & 0 & 0 & 0 & 0 & 0 \\ 0 & 0 & 0 & 0 & 0 & 0 \\ \gamma_{31} & 0 & 0 & 0 & 0 & 0 \\ \gamma_{41} & \gamma_{42} & 0 & 0 & 0 & 0 \\ \gamma_{51} = (1-\gamma_{31}-\gamma_{41}) & \gamma_{52} & \gamma_{53} & 0 & 0 & 0 \\ 0 & \gamma_{62} = (1-\gamma_{42}-\gamma_{52}) & \gamma_{63} & \gamma_{64} & 0 & 0 \end{bmatrix}$$

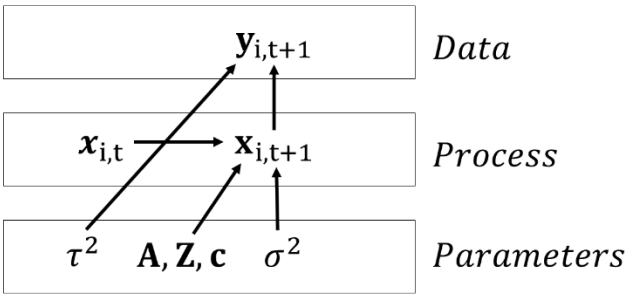


Figure 3: Directed acyclic graph of the density-independent models of this brown shrimp population. Solid arrows indicate a stochastic relationship between nodes, where nodes at the head of an arrow ($\boldsymbol{y}_{i,t+1}, \boldsymbol{x}_{i,t+1}$) are dependent on nodes at the tail of the arrow ($\boldsymbol{A}, \boldsymbol{Z}, \boldsymbol{c}, \sigma^2, \tau^2$) and nodes at the tail of an arrow must be expressed unconditionally with a probability distribution.

The density-independent models are specified by:

$$Pr\left[\mathbf{x}_{i,t+1}, \mathbf{x}_{i,t}, \mathrm{Z}, A, C, \sigma^2, \tau^2 \middle| \mathbf{y}_{i,t+1}\right] \tag{3}$$

$$\propto \prod_{t=1}^{T} N\left(\mathbf{y}_{i,t+1} \middle| \mathbf{x}_{i,t+1}, \tau^2\right) \times \prod_{t=1}^{T} N\left(\mathbf{x}_{i,t+1} \middle| (\mathbf{g}(\mathbf{Z}, \mathbf{A}, \mathbf{C}, \mathbf{x}_{i,t})), \sigma^2\right)$$

$$\times\ uniform(\mathrm{Z}|0,1)\ multinomial(\mathrm{A}|0,1)\ uniform(C|0,1e3)$$

$$\times\ uniform(\sigma^2|0.001,10)\ uniform(\tau^2|0.001,10)$$

and the density-dependent models are specified by:

$$Pr\left[\mathbf{x}_{i,t+1}, \mathbf{x}_{i,t}, \alpha, \beta, A, C, \sigma^2, \tau^2 \middle| \mathbf{y}_{i,t+1}\right] \tag{4}$$

$$\propto \prod_{t=1}^{T} N\left(\mathbf{y}_{i,t+1} \middle| \mathbf{x}_{i,t+1}, \tau^2\right) \times \prod_{t=1}^{T} N\left(\mathbf{x}_{i,t+1} \middle| (\mathbf{g}(\alpha, \beta, \mathbf{A}, \mathbf{C}, \mathbf{x}_{i,t})), \sigma^2\right)$$

$$\times\ uniform(\alpha|0,1)\ uniform(\beta|0,1e7)\ multinomial(\mathrm{A}|0,1)$$

$$\times\ uniform(C|0,1e3)\ uniform(\sigma^2|0.001,10)\ uniform(\tau^2|0.001,10)$$

### 2.5 The Bayesian Approach

The Bayesian approach treats all unknown quantities as random variables that take on a range of values rather than a single point estimate. This range of values is estimated by the posterior joint probability density function $p(\Theta|y)$ by finding the product of the maximum likelihood $L(\Theta|y)$ and the prior

distributions $p(\Theta)$, then dividing by the normalizing constant $p(y)$ (see Equation 5). Likelihood $L(\Theta|y)$ is proportional to the joint probability of observing the data 'y', given the parameters 'Θ', and can be viewed as a probability density function $\left(L(\Theta|y) \propto p(y|\Theta)\right)$.

$$p(\Theta|y) = \frac{p(y|\Theta)\, p(\Theta)}{p(y)} \tag{5}$$

All unknown parameters are random variables and are described by a prior distribution ($p(\Theta)$) representing knowledge about a particular parameter 'Θ' before considering the data 'y'. The normalizing constant $p(y)$ ensures the probability of all of the parameters, given the data, is equal to 1 ($\Sigma\, p(\Theta|y) = 1$). The unnormalized joint posterior distribution $p(\Theta|y)$ is proportional to the probability of obtaining the data, given the parameters $p(y|\Theta)$, times the prior $p(\Theta)$ (Ellison 1996; Hobbs and Hooten 2015). Because the normalizing constant is often impossible to calculate, I used a Monte Carlo Markov Chain (MCMC) sampling approach, which takes random draws from the marginal posterior distribution in proportion to their probability, producing a posterior distribution that is a probability density function with a total area equal to one. This is the key step that allows us to make probabilistic statements about parameters (Hobbs and Hooten 2015).

$$p(\Theta|y) \propto\ p(y|\Theta)\, p(\Theta) \tag{6}$$

**2.6 Prior Distributions**

All prior distributions in these analyses are the conjugates of the likelihood and all priors for unknown parameters were chosen to be as uninformative as possible in this study. Prior distributions and their parameters are summarized in the following section and in Table 2.

Observed population density ($Y_{t+1}$) was lognormally distributed, with mean = $x_{t+1}$ and observation error ($\varepsilon_t$). The true population density ($x_{t+1}$) was given as a lognormal distribution, with mean = $\mathbf{AZx}_{i,t} + c$ and process error ($\omega_t$). Initial population density ($x_0$) was given as a uniform distribution. Observation error variance ($\tau^2$) and process error variance ($\sigma^2$) have uniform prior distributions to indicate no prior knowledge of the true values of these parameters (Gelman 2006; Hobbs and Hooten 2015).

The probability an individual grows and subsequently transitions from stage i to stage j ($\gamma_{ji}$) was given as a multinomial distribution. The prior for $\gamma_{ji}$ was specified by a Dirichlet distribution, a multivariate generalization of the beta distribution used to model vectors of nonnegative random variables with their proportions summing to 1 (Gelman 2006; Hobbs and Hooten 2015; Rivot et al. 2004). The prior for $\gamma_{ji}$ is uninformative when all $a_j = 1$ for all $j$, giving all $\gamma_{ji}$ equal probability. These models simulated a multivariate draw using a series of binomial draws following the method described by Gelman et al. (2014).

The prior for density-independent survival ($\varphi_i$) was specified as a uniform distribution constrained between the values of 0 and 1. The prior for the maximum survival rate of stage i individuals at low densities ($\alpha_i$) in Beverton-Holt density-dependent survival (see "Density-Dependent Survival Models" in "Methods") was specified as a uniform distribution constrained between the values of 0 and 1. The prior for the strength of density-dependent mortality ($\beta_i$), i.e. how survival of stage $i$ individuals changes as density changes, was specified as a uniform distribution constrained between the values 0 and $10^7$, a large enough number to capture all plausible values. Priors for $\alpha_i$ and $\beta_i$ were weakly informative and flat to reflect no previous knowledge about the values of these parameters (Hobbs and Hooten 2015).

The prior for seasonal settlement was ($c_{is}$) specified as a uniform distribution constrained between the values 0 and 10,000. These constraints were based on the maximum number of individuals to recruit into a single stage in the dataset. All uniform priors were weakly informative and flat and therefore had little effect on the posterior distribution (Clark and Bjørnstad 2004; Hobbs and Hooten 2015). Posterior distributions were checked to ensure the specification of uninformative priors did not influence parameter estimates.

Table 2: Prior distributions for model parameters.

| Parameter | Definition | Prior |
|---|---|---|
| $x_0$ | Initial population density | $Uniform(1, 10^3)$ |
| $y_{i,t+1}$ | Observed population density | $lnorm(log(\boldsymbol{x}_{i,t+1}), \varepsilon_t)$ |
| $x_{i,t+1}$ | Unobservable true population density | $lnorm(log(\mathbf{AZ}\boldsymbol{x}_{\mathbf{i,t}} + \boldsymbol{c}_{i,s}),\ \omega_t)$ |
| $\sigma^2$ | Process variance | $Uniform(0.001,10)$ |
| $\tau^2$ | Observation variance | $Uniform(0.001,10)$ |
| $\varphi_i$ | Density-independent survival of an individual in stage i | $Uniform(0,1)$ |
| $\alpha_i$ | Maximum survival rate of stage i individuals at low densities in density-dependent survival | $Uniform(0,1)$ |
| $\beta_i$ | Strength of density-dependent mortality (how survival of stage i individuals changes as density changes) | $Uniform(0, 10^7)$ |
| $c_{is}$ | Proportion of individuals that settle into stage i in season s | $Uniform(0, 10^3)$ |
| $\gamma_{ji} = (\gamma_i, \gamma_j, \gamma_0 - \gamma_i - \gamma_j)$ | Probability an individual grows and subsequently transitions from stage i to stage j | $Dirichlet(1,1,1)$ |

### 2.7 Population Models

I tested six alternative models against the size and density-independent survival and growth (NULL) model. The alternative models describe survival as a function of:

1. Beverton-Holt density dependence,
2. stages affecting intraspecific competition (within a single stage or between all stages), and/or
3. presence of size-dependent survival.

Because of the risk of over-parameterization, I tested only one size-dependent growth model with density-independent survival. For all models, seasonal, stage-specific settlement was represented by the parameters $\Theta_{settle} = (c_{12}, c_{13}, c_{14}, c_{21}, c_{22}, c_{23}, c_{24}, c_{31}, c_{32}, c_{33}, c_{34})$, observation variance was estimated by the parameter $\tau^2$, and process variance was estimated by $\sigma^2$.

Table 3: Model description according to survival, growth and estimated parameters.

| Model | SURVIVAL | | | GROWTH | Parameters to estimate |
|---|---|---|---|---|---|
| | Density-Dependent | | Size-Dependent | Size-Dependent | |
| | Form | Competition | | | |
| NULL | - - - | - - - | - - - | - - - | $\Theta_{null} = (\varphi, \gamma_1, \gamma_2)$ |
| SDG | - - - | - - - | - - - | Size-Dependent | $\Theta_{SDG} = (\varphi, \gamma_{31}, \gamma_{41}, \gamma_{42}, \gamma_{52}, \gamma_{53}, \gamma_{63}, \gamma_{64})$ |
| SDS | - - - | - - - | Size-Dependent | - - - | $\Theta_{SDS} = (\varphi_1, \varphi_2, \varphi_3, \varphi_4, \gamma_1, \gamma_2)$ |
| BW | Beverton Holt | Within single stage | - - - | - - - | $\Theta_{BW} = (\alpha_1, \beta_1, \gamma_1, \gamma_2)$ |
| BWS | Beverton Holt | Within single stage | Size-Dependent | - - - | $\Theta_{BWS} = (\alpha_1, \beta_1, \alpha_2, \beta_2, \alpha_3, \beta_3, \alpha_4, \beta_4, \gamma_1, \gamma_2)$ |
| BA | Beverton Holt | Between all stages | - - - | - - - | $\Theta_{BA} = (\alpha_1, \beta_1, \gamma_1, \gamma_2)$ |
| BAS | Beverton Holt | Between all stages | Size-Dependent | - - - | $\Theta_{BAS} = (\alpha_1, \beta_1, \alpha_2, \beta_2, \alpha_3, \beta_3, \alpha_4, \beta_4, \gamma_1, \gamma_2)$ |

### *2.7.1 Size-Independent and Density-Independent Survival and Growth (NULL model)*

The null model (NULL) assumes survival is constant across all stages so $\varphi = \varphi_1 = \varphi_2 = \varphi_3 = \varphi_4$ (matrix $\boldsymbol{Z}$) and growth $\gamma_{ji}$ (matrix $\boldsymbol{A}$) does not depend on size or density. For example, the probability of growing 20-30 mm is equal across stages and estimated by $\gamma_1$ where $\gamma_1 = \gamma_{31} = \gamma_{42} = \gamma_{53} = \gamma_{64}$ (matrix $\boldsymbol{A}$). Likewise, the probability of growing 31-40 mm is equal across stages so, $\gamma_2 = \gamma_{41} = \gamma_{52} = \gamma_{63}$ and the probability of growing 41 mm or more ($\gamma_3$) is estimated by $(1 - \gamma_1 - \gamma_2)$. The parameters for this model are listed in Table 3.

### *2.7.2 Size-Dependent Growth (SDG model)*

The SDG model assumes survival is constant across all stages where $\varphi = \varphi_1 = \varphi_2 = \varphi_3 = \varphi_4$ (matrix $\boldsymbol{Z}$), while growth depends on the individual's originating stage (matrix $\boldsymbol{A}$). The parameters for the SDG model are listed in Table 3.

### *2.7.3 Size-Dependent Survival (SDS model)*

The SDS model assumes survival depends on an individual's originating stage, while growth does not depend on stage where $\gamma_1 = \gamma_{31} = \gamma_{42} = \gamma_{53} = \gamma_{64}, \gamma_2 = \gamma_{41} = \gamma_{52} = \gamma_{63}$ and $\gamma_3 = (1 - \gamma_1 - \gamma_2)$ (matrix $\boldsymbol{A}$). The parameters for the SDS model are listed in Table 3.

### *2.7.4 Density-Dependent Survival Models*

The density-dependent survival models assume survival depends on density but not on an individual's originating stage. The Beverton-Holt models estimate stage-specific survival with

$\varphi_i = \frac{\alpha_i}{1+\beta_i x_n}$ where $\alpha_i$ = the maximum survival rate reached at low densities in stage *i* and $\beta$ = the strength of density dependence on mortality or how survival of stage *i* decreases as density increases within or between stages (Beverton and Holt 1954). Density dependence results from competition for limited resources either within a single stage or between all stages. In models where survival is a result of competition within a single stage only, $x_i$ = the density of individuals in the stage for which survival ($\varphi_i$) is being estimated at time $t$. In models where survival is a result of competition between all stages, $x_n = (x_1 + x_2 + x_3 + x_4 + x_5 + x_6)$, that is, survival is a function of the density of shrimp in all stages at time $t$. The former model is denoted BW and the latter model BA. If $\beta = 0$, no density dependence is present, if $\beta > 0$, compensatory density dependence is present (Beverton and Holt 1954). Parameters are constrained within reasonable values, so that $0 \leq a \leq 1$ and $0 \leq \beta$. Parameters to be estimated for the Density-Dependent Survival models BW and BA are listed in Table 3.

### *2.7.5 Size and Density-Dependent Survival Models*

Size and Density-dependent models assume growth does not depend on size or density but survival nonetheless depends on an individual's originating stage and density of that stage (within stage competition) or the density of all stages (between stage competition). The Beverton-Holt survival equation for competition within a single stage estimates stage-specific survival where $\varphi_1 = \frac{\alpha_1}{1+\beta_1 x_1}$, $\varphi_2 = \frac{\alpha_2}{1+\beta_2 x_2}$, $\varphi_3 = \frac{\alpha_3}{1+\beta_3 x_3}$, and $\varphi_4 = \frac{\alpha_4}{1+\beta_4 x_4}$. Again, in models where survival is a result of competition between all stages, $x_n = (x_1 + x_2 + x_3 + x_4 + x_5 + x_6)$. Parameters for the size and density-dependent models, denoted BWS and BAS, are listed in Table 3.

## 2.8 Convergence Diagnostics

To estimate the posterior joint pdf, I used JAGS (Plummer 2003) called from R (R Core Team 2015) with package "rjags" to implement a Markov Chain Monte Carlo (MCMC) sampling approach. For each model I ran three or seven independent chains with different initial values for all monitored parameters with a burn-in of 6000 iterations and a thinning rate of 1 in 100 until convergence was achieved.

Convergence indicates that sufficient samples have been drawn from the MCMC to accurately define the posterior distribution of that parameter so that the distribution becomes stationary over MCMC simulation (Kruschke 2014). I determined convergence according to the potential scale reduction factor (psrf), a Gelman-Rubin diagnostic statistic that compares variance between chains and variance within a chain,

and shows convergence when these variances are approximately equal (Gelman and Rubin 1992; Hobbs and Hooten 2015). I ran all models until the Gelman-Rubin statistic for all parameters was below 1.05, indicating convergence. To determine if MCMC chains were long enough for parameter estimates to be stable and accurate, I evaluated trace plots and density plots, looking for overlapping chains with no orphan chains (Hobbs and Hooten 2015; Kruschke 2014). See Appendix A for convergence diagnostics for all parameters.

### 2.9 Model Selection

I used deviance information criteria (DIC) to evaluate model fit (Spiegelhalter et al. 2002). DIC is a Bayesian alternative to Akaike's information criteria (AIC). DIC is calculated by summing the mean deviance, a loss function that is a measure of fit, and the penalty (pD) for the model, which estimates the effective number of parameters and is a measure of model complexity (Hobbs and Hooten 2015; Kruschke 2014; Spiegelhalter et al. 2002). DIC is most appropriate for model selection when models are linear and the number of parameters is much greater than the number of independent observations (Hooten and Hobbs 2015; Plummer 2008).

# 3. RESULTS

I evaluated model convergence according to the Gelman Rubin statistic (psrf). The size-independent survival and growth (NULL), size-dependent growth (SDG), size-dependent survival (SDS), within-stage Beverton-Holt density dependence (BW) and between-stage Beverton-Holt density dependence (BA) models converged. Models incorporating both density dependence survival and size-dependent growth (BWS and BAS) did not converge, suggesting overparamaterization of those models (Table 4).

Table 4: Model ranks according to deviance information criteria (DIC).

| MODEL | MODEL DESCRIPTION | RESULTS | | |
|---|---|---|---|---|
| | | MEAN DEVIANCE | PENALTY (pD) | PENALIZED DEVIANCE (DIC) |
| SDS | Size-dependent survival | 3563 | 520.9 | 4084 |
| BW | Within stage density-dependent survival | 4148 | 189.5 | 4337 |
| BA | Between all stages density-dependent survival | 4533 | 108.5 | 4642 |
| NULL | Size and density-independent survival and growth | 3577 | 1271 | 4848 |
| SDG | Size-dependent growth | 3396 | 2885 | 6281 |
| BWS | Within stage density-dependent survival and size-dependent growth | Did not converge after 23 weeks | | |
| BAS | Between all stages density-dependent survival and size-dependent growth | Did not converge after 20 weeks | | |

I evaluated autocorrelation plots and effective sample size (ESS). Autocorrelation indicates the dependence of one MCMC sample on the previous MCMC sample, where high autocorrelation indicates the MCMC samples may be unrepresentative of the posterior distribution (Hobbs and Hooten 2015). Autocorrelation was high for process variance and observation variance in all models and alpha and beta in density-dependent models. To address this high autocorrelation, I reported median values for all parameters, because the median is less influenced by sparse regions of the highest density interval (HDI) and these sparse regions are less sufficiently sampled when autocorrelation is high (Kruschke 2014). Kruschke (2014) recommends a minimum ESS of 10,000 to ensure accurate parameter estimates,

especially for estimates that depend on the limits of the HDI, such as with $\beta$. ESS for $\beta$ on the BW model was >10,000 and therefore, the limits of the HDI are an accurate estimate (Figure 4). The ESS for $\beta$ on the BA model, however, was 232.4 (Figure 5). This low ESS indicates that the limits of the HDI may not be accurate; consequently, I drew conclusions about density dependence based solely on the BW model (Kruschke 2014). See Appendix A for trace, autocorrelation and density plots for all parameters.

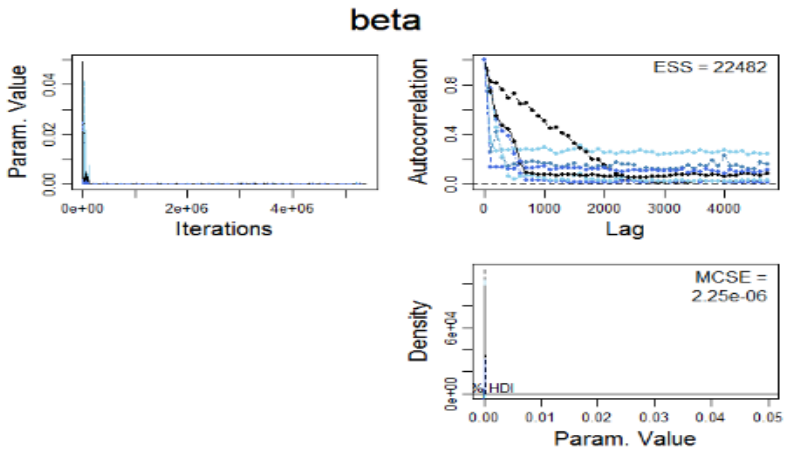


Figure 4: Within stage density-dependent survival (**BW**) convergence diagnostics for β. Trace plot (top left), autocorrelation plot with effective sample size (ESS) (top right) and density plot with Monte Carlo Standard error (MCSE).

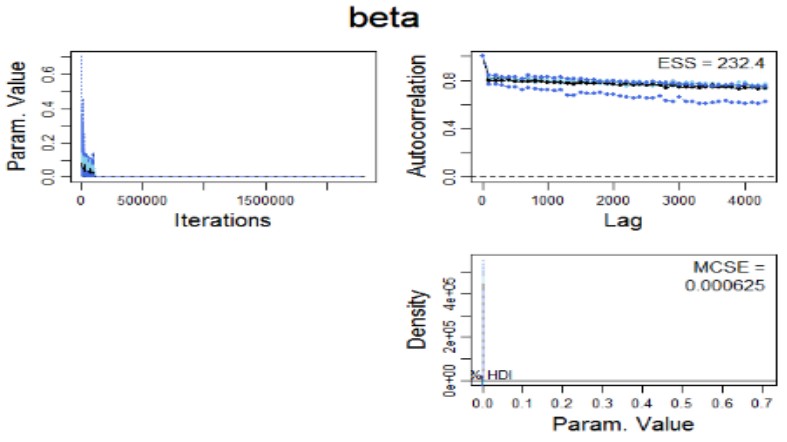


Figure 5: Between all stages density-dependent survival (**BA**) convergence diagnostics for β. Trace plot (top left), autocorrelation plot with effective sample size (ESS) (top right) and density plot with Monte Carlo Standard error (MCSE).

Finally, models were compared using deviance information criteria (DIC). Overall, DIC for all models was high, indicating poor fit (Spiegelhalter et al. 2002) (Table 4). This poor fit was expected, however, given that I did not incorporate any of the important environmental factors known to affect brown shrimp survival and growth in the juvenile stage. The best-fit model according to DIC was the size-dependent survival (SDS) model (DIC 4084). The second-best model was the within-stage density-dependent survival (BW) model (DIC 4337), followed by the between-all-stages density-dependent survival (BA) model (DIC 4642). The worst-fit models were the size and density-independent survival and growth (NULL) model (DIC 4848) and the size-dependent growth (SDG) model (DIC 6281) (see Table 4).

Some values were highly autocorrelated, fit was low in all models and environmental variables were not included explicitly in these analyses. Therefore, conclusions should only be drawn about model selection, and the actual values of parameters should be considered with caution. With these considerations in mind, I report the median of each estimated parameter (Figure 6 – Figure 11) and the 95% HDI for each parameter, which gives the most credible parameter values with a 95% total probability. See Appendix B for posterior distributions for all parameters.

### 3.1 Parameter Comparisons

Median survival in stage 1 ($\varphi_1 = 0.215$) of the SDS model, survival in all stages in the NULL ($\varphi = 0.171$) and SDG ($\varphi = 0.189$) models, and the maximum survival rate at low densities in the BW ($\alpha_1 = 0.193$) and BA ($\alpha_1 = 0.189$) models were within 0.044 of each other. (Figure 6). In the best-fit model (SDS), survival in subsequent stages past stage 1 was lower than survival in stage 1. In both density-dependent survival models (BW, BA), the HDI for $\beta$ did not include zero (Figure 7, Figure 8 respectively).

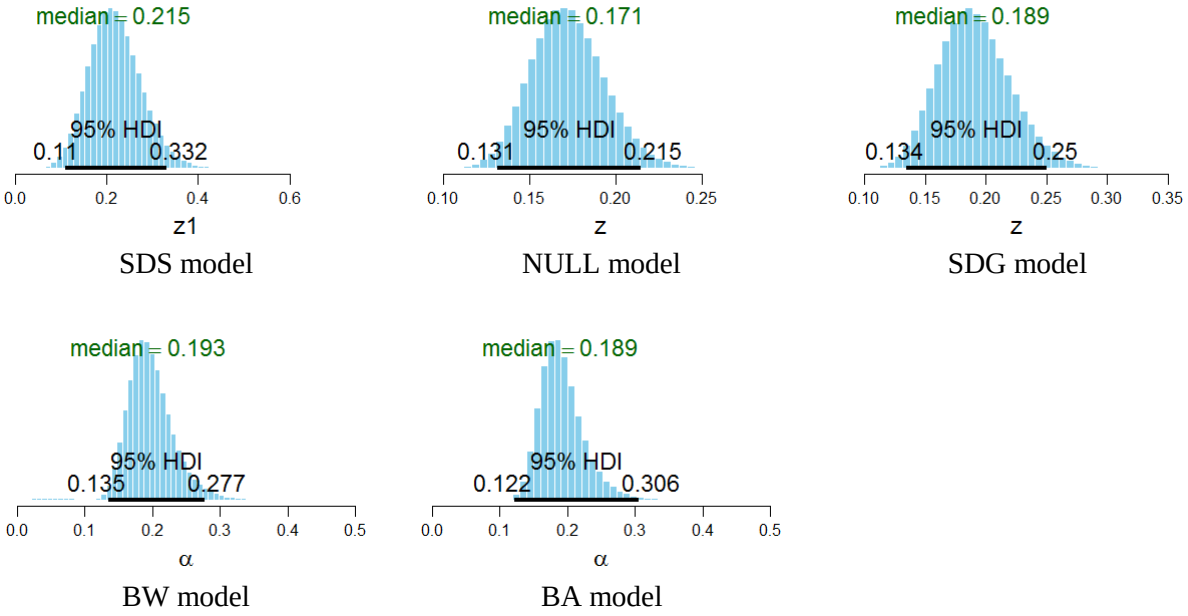


Figure 6: Median and 95% highest density interval (HDI) for survival in all models. In density-independent models (SDS, NULL, SDG) survival ($\varphi_i$) estimates the probability of survival in stage i, while survival in density-dependent models (BW, BA) estimates $\alpha_1$, maximum survival rate of at low densities, and $\beta_1$, strength of density-dependent mortality.

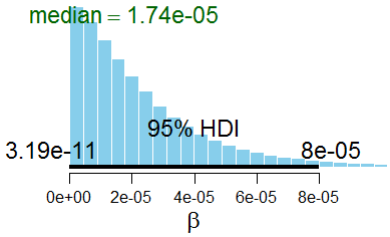


Figure 7: Within stage density-dependent survival (**BW**) 95% HDI for β indicates density dependence in the population.

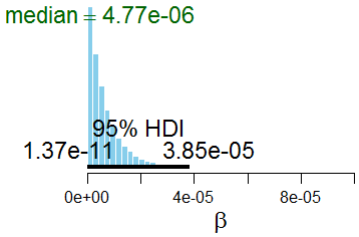


Figure 8: Between all stages density-dependent survival (**BA**) 95% HDI for β indicates density dependence in the population, however convergence diagnostics indicates poor mixing and a non-stationary distribution.

The median probability of growing 20 – 30 mm in the SDS model ($\gamma_1 = 0.636$), BW model ($\gamma_1 = 0.662$), BA model ($\gamma_1 = 0.659$) and NULL model ($\gamma_1 = 0.652$), all were within 0.023 of each other. The median probability of growing 31 - 40 mm in the SDS model ($\gamma_2 = 0.24$), BW model ($\gamma_2 = 0.220$), and BA model ($\gamma_2 = 0.224$), were within 0.020 of each other. The median probability of growing 31 - 40 cm in the NULL model ($\gamma_2 = 0.418$) was much higher than all other models. Finally, the median probability of 41 mm or more in the SDS model ($\gamma_3 = 0.124$), BW model ($\gamma_3 = 0.118$), and BA model ($\gamma_3 = 0.117$) were within 0.007 of each other. The median probability of growing 41 mm or more in the NULL model ($\gamma_3 = 0.500$) was much higher than all other models (Figure 9). The SDG model was not included in the comparison of growth parameters because the parameters estimated in this model were not comparable to other models since growth in the SDG model was stage-specific.

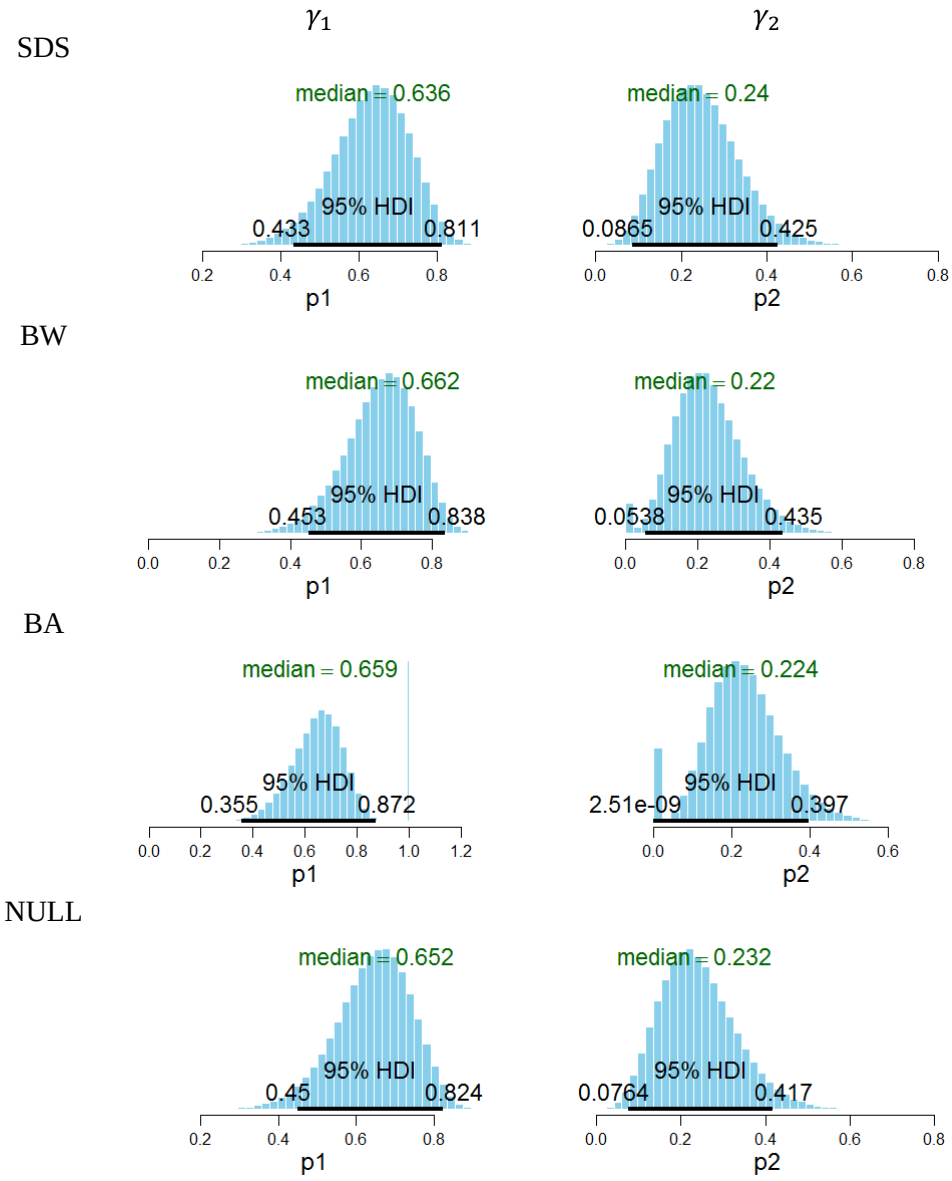


Figure 9: Median and 95% highest density interval (HDI) for probability of growing 20 – 30 mm ($\gamma_1$) and the probability of growing 31 - 40 mm ($\gamma_2$). The median probability of growing 4 mm or more ($\gamma_3$) = 1 - $\gamma_1 - \gamma_2$ is confounded with emigration.

Median observation variance in the SDS model ($\tau^2 = 0.009$), BW model ($\tau^2 = 0.038$), and BA model ($\tau^2 = 0.056$) were low, indicating a sufficient sample size, and were within 0.047 of each other. Median observation variance in the NULL model ($\tau^2 = 0.0919$) and the SDG model ($\tau^2 = 0.13$) were about double those previously stated (Figure 10). Median process variance in all models was high, which was expected given that I did not incorporate any density-independent factors in the models tested. Median process variance for the SDS model ($\sigma^2$ = 1.12), BW model ($\sigma^2$ = 1.11), BA model ($\sigma^2$ = 1.09), NULL model ($\sigma^2$ = 1.03) and SDG model ($\sigma^2$ = 0.995) were all within 0.125 each other (Figure 11).

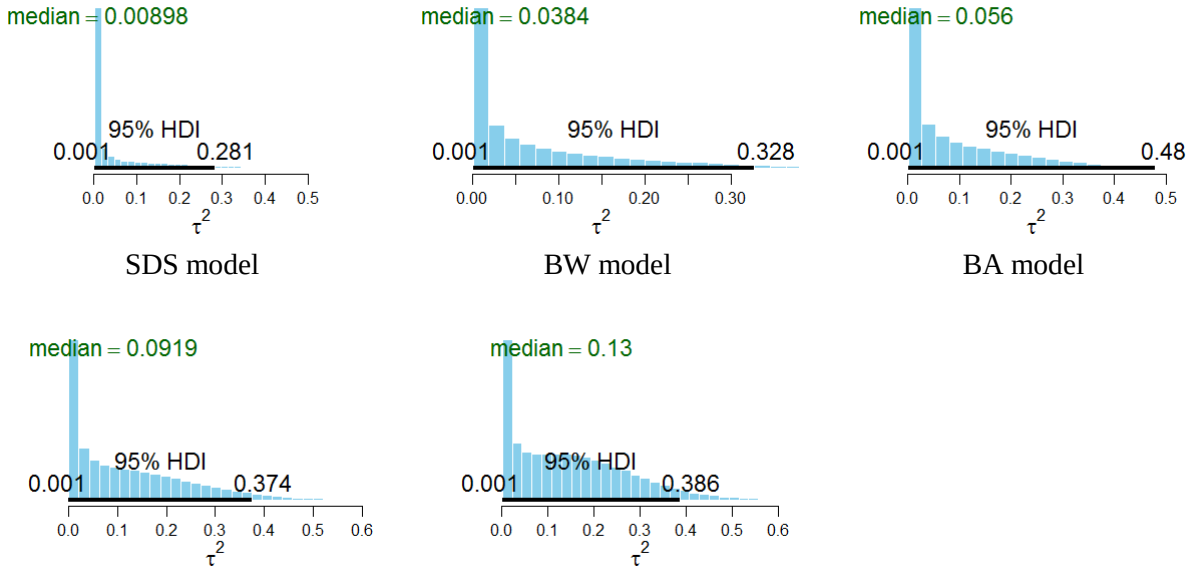


Figure 10: Median and 95% highest density interval (HDI) for observation error variance ($\tau^2$) in all models.

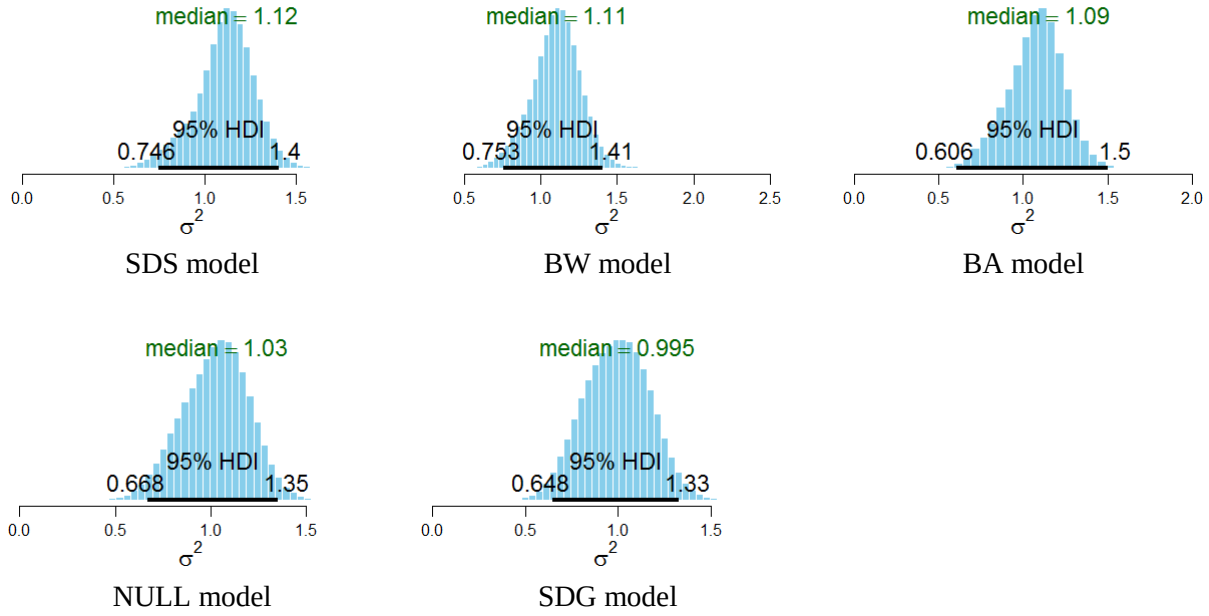


SDS model BW model BA model

NULL model SDG model

Figure 11: Median and 95% highest density interval (HDI) for process error variance ($\sigma^2$) in all models.

# 4. CONCLUSION

Using Bayesian state space matrix population models, I tested for size-dependent survival (SDS), size-dependent growth (SDG), within-stage Beverton-Holt density-dependent survival (BW), between all stages Beverton-Holt density-dependent survival (BA), and size and density-independent survival and growth (NULL). My results indicate that size-dependent survival was the most important factor acting on the juvenile stage of this population, that density-dependent survival is present in the juvenile stage of this population, and that evidence was weak for size and density-independent survival and growth. Finally, my analyses show that the size-dependent growth (SDG) model was the worst-fitting model among those tested, which I hypothesize is a result of the assumption made in this model that survival was both size and density-independent.

## 4.1 Size-Dependent Models

My analyses show that the size-dependent survival (SDS) model was the best fit and, consequently, that size-dependent survival was the strongest force acting on this juvenile brown shrimp population. These results support the well-known importance of size on survival where increased size leads to increased survival rates in fish (Anderson 1988; Houde 1987; Shepherd and Cushing 1980; Ware 1975) and brown shrimp (Minello et al. 1989). Theory suggests that increased survival results from an individual's improved ability to exploit resources (Cowan Jr et al. 1997; Werner and Gilliam 1984), make fewer risky foraging decisions (Cowan Jr et al. 1997; Houde 1997; Mangel and Clark 1988) escape predation from gape-limited predators (Anderson 1988; Minello et al. 1989; Sogard 1997; Ware 1975; Werner and Gilliam 1984), and reduced vulnerability to starvation and environmental extremes with increasing size (Sogard 1997).

These results, however, do not necessarily show the expected mechanism driving the relationship between size and survival. This is likely because survival rates in all but stage 1 are confounded with emigration. For example, if an individual in stage 2 grows 41 or more mm in a single time step, that individual could transition to stage 6 or greater and recruit offshore. Future analyses could attempt to account for emigration rates by monitoring movement of subadult from estuaries into open bays, however this has proven difficult in the past.

Simpson's paradox (Simpson 1951) offers another potential explanation for the discrepancy between my results and theory. This paradox is a statistical phenomenon where trends, such as rates, may show one trend when groups of data are separated, but may show a different trend when groups of data are aggregated. My data were grouped across cohort, season, environmental condition and habitat type, any of which may have resulted in Simpson's paradox. Future analyses should incorporate season, environmental conditions and habitat type as grouping variables to investigate these results further and to improve the model.

I compared past estimates of natural brown shrimp mortality to parameter estimates from my size-dependent survival (SDS) model. Minello et al. (1989) estimated juvenile brown shrimp densities, using a drop-sampling technique to capture brown shrimp during spring flood tides at 2-week intervals in a Galveston Bay estuary. Brown shrimp were then classified according to size class. Minello et al. (1989) identified a mean two-week survival rate of 0.58 in cohorts with mean lengths between 18.2 – 30.8 mm, mean two-week survival of cohorts with mean lengths between 30.8 – 45.2 mm was 0.61 and mean two-week survival of cohorts with mean lengths between 45.2 – 62.8 mm was 0.99. The mean two-week survival for both cohorts examined over both years (1982 and 1987) was 0.39. Minello et al. (1989) found that these survival rates varied considerably between cohorts and between years and determined that survival would change with habitat availability. McCoy (1972) found two-week survival rates of North Carolina subadult brown shrimp to be 0.48. These previously published survival rates are much higher than survival parameters identified in my SDS model (Table 5). This large difference in estimated survival is not unexpected given that survival rates in these analyses were confounded with recruitment. In addition, Minello et al. (1989) evaluated survival rates for four cohorts separately whereas I used likelihood to determine median rates for many cohorts over 11 years in all seasons, during which environmental conditions and access to vegetated marsh, which influences survival independent of size, likely varied considerably (Haas et al. 2001; Minello et al. 1989; Rozas and Minello 2011; Zein-Eldin and Griffith 1967; Zein-Eldin and Renaud 1986).

Table 5: Comparison of survival rates from (Minello et al. 1989) and this study.

| Minello et al. (1989) (mean two-week survival of a single cohort (82A) from life table analysis) | | This study (median monthly survival from SDS model using Bayesian state space modeling) | |
|---|---|---|---|
| mean cohort length | survival | cohort length | survival |
| 18.2 – 30.8 mm | 0.58 | 10 – 20 mm | 0.215 |
| | | 21 – 30 mm | 0.160 |
| 30.8 – 45.2 mm | 0.61 | 31 – 40 mm | 0.129 |
| 45.2 – 62.8 mm | 0.99 | 41 – 50 mm | 0.193 |

The size-dependent growth (SDG) model had the worst fit among the models tested. Size-dependent growth, however, was expected to be important in this brown shrimp population because growth, size, and survival are intricately linked (Ware 1975). Theory suggests that slower growth leads to prolonged stage duration and higher susceptibility to predation (Anderson 1988; Houde 1987; Houde 1997; Werner and Gilliam 1984), but faster growth results in less time spent in smaller stages, leading to increased survival (Minello et al. 1989). Consequently, growth must have strong positive influences on size-dependent survival of brown shrimp (Anderson 1988; Ware 1975; Werner and Gilliam 1984) or *vice versa* by selecting the individuals that grow faster which changes the apparent growth rate. Because my results show that size-dependent survival is the most important force acting on the population, followed by density-dependent survival, I believe that my assumption that survival is not dependent on size or density in the SDG model likely reduced the model's predictive ability, leading to poor model fit.

Table 6: Brown shrimp growth rates from past studies.

| Juvenile growth rate (mm/day) | Reference | Season of study | Description of study and growth estimate |
|---|---|---|---|
| 0.43 – 1.67 | Loesch (1965) | November - May | *In situ* growth estimates in an Alabama estuary. |
| 0.5 – 1.7 | Minello et al. (1989) | spring | Mean growth calculated from mean lengths of cohorts. |
| 0.7 – 1.9 | Rozas and Minello (2009) | spring and summer | Mean growth rates in 4 habitat type treatments. |
| 0.6 – 1.2 | Rozas and Minello (2011) | May and September | Experimental treatment of a range of and combinations of salinity and water temperatures. |
| 1.53 | Williams (1955) | warmer months | *In situ* growth estimates in a Louisiana brackish estuary. |
| 1.7 | St Amant et al. (1963) | March, April, May | *In situ* growth estimates in a Louisiana estuary. |
| 0.77 – 1.41 | Minello and Zimmerman (1991) | summer | Caged experiments in vegetated and non-vegetated habitat at low and high shrimp densities. |

Past brown shrimp growth studies focus on average growth in millimeters per day or growth in extreme environmental conditions, rather than probability of growing a given amount over a given time period. Consequently, it is difficult to compare my growth parameters to published values. We know, however, that published juvenile growth rates have ranged from 0.43 – 1.9 mm/day (see Table 6) (Loesch 1965; Minello and Zimmerman 1991; Minello et al. 1989; Rozas and Minello 2009; Rozas and Minello 2011; St Amant et al. 1963; Williams 1955), and these rates encompass all growth rates I considered plausible in these analyses (0.67 – 1.3 or more mm/day) supporting the assumption that my analyses employed biologically reasonable growth rates. However, if minimum growth rates observed in past studies (0.43 mm/day) were constant for 30 days, brown shrimp could potentially grow as little as 12.9 mm in a time step. Future models should adjust these assumed minimum growth of 20 mm/30 days to this lower rate, particularly when environmental conditions likely lead to slower growth.

### 4.2 Density-Dependent Models

Although the SDS model was the best-fit model, my density-dependent models (BW, BA) fit better than the NULL and SDG models, with BW fitting better than BA. Parameter β in the BW model had a median of 1.74E-05 with a low HDI limit that did not include zero, indicating the presence of within stage density

dependence in the juvenile stage of this population. Parameter β in the BA model, however, had a small ESS, so I did not interpret the limits of the 95% HDI (Kruschke 2014). I was unable to test models that incorporated both size and density dependence due to convergence issues. Future analyses should repeat my attempt to combine size and density-dependent survival into a single model to determine if the combined effects of size and density on survival provide a better fit model then size-dependent survival alone.

Predation is an important source of mortality in the early life stages of most fish (Bailey and Houde 1989; Werner and Gilliam 1984), and it is the major source of post larval and juvenile brown shrimp mortality in estuaries (Divita et al. 1983; Minello et al. 1989; Nance 1989). Brown shrimp escape predation pressure in marshes (Boesch and Turner 1984) where vegetative structure provides a refuge from predatory fishes (Kneib 1995; Minello and Wooten Jr 1993; Minello and Zimmerman 1991; Minello et al. 1989; Roth et al. 2008). Some predators, such as southern flounder, pinfish and Atlantic croaker, are negatively impacted by the presence of vegetation, while others are unaffected (Minello and Zimmerman 1983; Minello et al. 1989). Because the importance of vegetated marsh changes with the predator species present, the strength of density dependence may change considerably with a changing predator assemblage. To account for these changes, future analyses could be improved by incorporating predator species presence and abundance.

Brown shrimp select vegetated marsh edge, where their benthic infaunal prey (Gleason and Wellington 1988; Kneib 1984; McTigue and Zimmerman 1998; Minello et al. 1994) are most abundant (Minello and Zimmerman 1991; Rader 1984; Riera et al. 2000; Rozas and Zimmerman 2000; Whaley 1997; Whaley and Minello 2002). Increased foraging opportunities at the marsh edge (McTigue and Zimmerman 1998; Rozas and Odum 1988) contributes to increased growth rates in brown shrimp at marsh edge (Cowan Jr et al. 1997). Minello and Zimmerman (1991) found that brown shrimp growth rates decreased with increasing densities in the presence of *Spartina alterniflora* in a cage experiment. If marsh, which harbors prey, is limited, increasing densities of brown shrimp should lead to decreasing consumption rates and decreasing growth for those individuals not in optimal habitat, resulting in density-dependent growth and survival (Sissenwine 1984; Ware 1975). To test for the presence of density-dependent growth by means of this mechanism, future analyses should incorporate prey abundance and availability by habitat type.

Brown shrimp select marsh edge to minimize the risk of stranding (Kneib and Wagner 1994; Kneib 1984; Minello et al. 2012), for refuge from predation (Boesch and Turner 1984; Kneib 1995; Minello and

Wooten Jr 1993; Minello and Zimmerman 1991; Minello et al. 1989; Roth et al. 2008), and for increased access to infaunal prey (Cowan Jr et al. 1997; McTigue and Zimmerman 1998; Rozas and Odum 1988). But marsh edge is only accessible when flooded (Minello et al. 2015). Competition for marsh, therefore, can only occur when brown shrimp have access to marsh, and density-dependent effects on survival and growth can only occur when this competition is present. Consequently, the value of marsh changes with duration and extent of tidal inundation (Baker et al. 2013) which can be highly variable in Galveston Bay, especially over short time scales (Hicks et al. 1983; Minello et al. 2015; Rozas 1995; Turner 1991). To account for this high variability, Rozas et al. (2007) collected samples that yielded data for my study during periods when both marsh and nonvegetated bottom were submerged <1m deep. To improve our ability to detect density dependence in the presence of this highly variable environment and to determine the magnitude of compensation, future analyses should incorporate flooding duration and tidal inundation.

### 4.3 Density-Independent Factors

Growth and survival are affected by density-independent environmental factors, including temperature and salinity. Higher temperatures increase growth rates (Anderson 1988; Haas et al. 2001; Sissenwine 1984) with postlarval and juvenile brown shrimp growing most rapidly, between 11℃ and 32.5℃ (Zein-Eldin and Aldrich 1965; Zein-Eldin and Griffith 1966; Zein-Eldin and Griffith 1967), and growth declining sharply at temperatures above 35℃ (Zein-Eldin and Griffith 1967). Brown shrimp survival rates decreased at temperatures over 27.5℃ (Zein-Eldin and Renaud 1986) and resulted in 100% mortality at temperatures over 35℃ (Zein-Eldin and Griffith 1966; Zein-Eldin and Griffith 1967). The influence of salinity is less clear than that of temperature because effects on growth and survival likely result from a combination of higher metabolic costs and reduced prey abundance at low salinities (Rozas and Minello 2011; Zimmerman et al. 1990). Rozas and Minello (2011) found no significant difference in survival at various salinities, although survival of postlarval and juvenile brown shrimp decreases from combinations of either low temperature (11℃-15℃) or high temperature (over 30℃) and low salinity (5%) (Zein-Eldin and Aldrich 1965; Zein-Eldin and Renaud 1986). Experimental and modeling studies determined that brown shrimp prefer mesohaline (5-18 ppt) and polyhaline (18-30 ppt) conditions (Clark et al. 2004; Doerr et al. 2016; Rozas and Reed 1994) and that their growth rates are lower in oligohaline conditions (0.5-5 ppt) and higher in mesohaline conditions (Rozas and Minello 2011; Saoud and Davis 2003).

These density-independent environmental factors were not explicitly represented in these models, but rather the effects of salinity, temperature, and other processes were represented by the process variance parameter estimated for each model. As expected, because of the significant influence of these

environmental conditions on juvenile brown shrimp (Minello and Rozas 2002; Rosas et al. 1999; Rozas and Minello 2011; Rozas and Zimmerman 2000; Saoud and Davis 2003; Zein-Eldin and Aldrich 1965; Zein-Eldin and Renaud 1986; Zimmerman and Minello 1984; Zimmerman et al. 1984) and the high variability of these environmental conditions (Fogarty et al. 1991; Rozas et al. 2007), process variance was large in all models, ranging from 0.995 – 1.119 (see Table 5), much higher than observation variance which ranged from 0.009 – 0.130. When process error is high compared to observation error, this tells us that the model has little predictive value (Hobbs and Hooten 2015). To reduce process error, the models would need to be improved (Hobbs and Hooten 2015), which could be accomplished by incorporating environmental factors as predictive covariates. Again, this lack of fit and low predictive power in all models tested indicates that parameter values should be viewed with caution.

This study was a first step toward identifying the presence and mechanisms driving compensation in brown shrimp. I estimated that size-dependent survival was the strongest force acting on the juvenile stage of this brown shrimp population and that density dependence is present in the juvenile stage. Detection of density dependence in the juvenile stage suggests that this could be the regulatory stage in the life cycle. Future analyses should aim to quantify the magnitude and mechanisms of compensation acting on juvenile brown shrimp by incorporating predator presence and abundance, prey abundance and availability and flooding duration and tidal inundation into future models. To improve the predictive value of future models, salinity and temperature should be included as covariates. Future analyses should also attempt to combine size and density dependence into a single model to determine if the joint effect of size and density on survival or growth better explains the juvenile stage compared to size or density alone. By identifying the magnitude and mechanisms of compensation acting on juvenile brown shrimp, managers will be able to predict harvest abundance more accurately and better understand how impending habitat losses may affect shrimp abundance long-term should habitat become a more limited resource (Haas et al. 2001; Minello and Zimmerman 1991).

# REFERENCES


Anderson, J. T. 1988. A review of size dependent survival during pre-recruit stages of fishes in relation to recruitment. Journal of Northwest Atlantic Fishery Science 8:55-66.

Bailey, K., and E. Houde. 1989. Predation on eggs and larvae of marine fishes and the recruitment problem. Advances in Marine Biology 25:1-83.

Baker, R., B. Fry, L. P. Rozas, and T. J. Minello. 2013. Hydrodynamic regulation of salt marsh contributions to aquatic food webs. Marine Ecology Progress Series 490:37-52.

Baxter, K., and L. Sullivan. 1986. Forecasting offshore brown shrimp catch from early life history stages. Pages 22-36 *in* Proceedings of the Shrimp Yield Prediction Workshop. Texas A&M Sea Grant Publication, TAMU–SG–86–110. College Station, Texas.

Baxter, K. N., and W. C. Renfro. 1967. Seasonal occurrence and size distribution of postlarval brown and white shrimp near Galveston, Texas, with notes on species identification. Fishery Bulletin 66(1).

Beverton, R. J., and S. J. Holt. 1954. On the dynamics of exploited fish populations, volume 11. Springer Science & Business Media.

Boesch, D. F., and R. E. Turner. 1984. Dependence of fishery species on salt marshes: the role of food and refuge. Estuaries and Coasts 7(4):460-468.

Brännström, Å., and D. J. Sumpter. 2005. The role of competition and clustering in population dynamics. Proceedings of the Royal Society of London B: Biological Sciences 272(1576):2065-2072.

Brook, B. W., and C. J. Bradshaw. 2006. Strength of evidence for density dependence in abundance time series of 1198 species. Ecology 87(6):1445-1451.

Childers, D., J. Day, and R. Muller. 1990. Relating climatological forcing to coastal water levels in Louisiana estuaries and the potential importance of El Nino-Southern Oscillation events. Climate Research 1(1):31-42.

Clark, J. S., and O. N. Bjørnstad. 2004. Population time series: process variability, observation errors, missing values, lags, and hidden states. Ecology 85(11):3140-3150.

Clark, R. D., and coauthors. 2004. A habitat-use model to determine essential fish habitat for juvenile brown shrimp (*Farfantepenaeus aztecus*) in Galveston Bay, Texas. Fishery Bulletin 102(2):264-277.

Cook, H. L., and M. J. Lindner. 1970. Synopsis of biological data on the brown shrimp, *Penaeus aztecus Ives*, 1891. Bureau of Commercial Fisheries, Galveston, Texas 77550, USA.

Cowan Jr, J. H., K. A. Rose, and E. D. Houde. 1997. Size-based foraging success and vulnerability to predation: selection of survivors in individual-based models of larval fish populations. Pages 357-386 *in* Early Life History and Recruitment in Fish Populations. Springer.

Cushing, D. 1990. Plankton production and year-class strength in fish populations: an update of the match/mismatch hypothesis. Advances in Marine Biology 26:249-293.

de Valpine, P., and A. Hastings. 2002. Fitting population models incorporating process noise and observation error. Ecological Monographs 72(1):57-76.

Dennis, B., J. M. Ponciano, S. R. Lele, M. L. Taper, and D. F. Staples. 2006. Estimating density dependence, process noise, and observation error. Ecological Monographs 76(3):323-341.

Divita, R., M. Creel, and P. Sheridan. 1983. Foods of coastal fishes during brown shrimp, *Penaeus aztecus*, migration from Texas estuaries. Fishery Bulletin 81(2):396 - 404.

Doerr, J. C., H. Liu, and T. J. Minello. 2016. Salinity selection by juvenile brown shrimp (*Farfantepenaeus aztecus*) and white shrimp (*Litopenaeus setiferus*) in a gradient tank. Estuaries and Coasts 39(3):829-838.

Ellison, A. M. 1996. An introduction to Bayesian inference for ecological research and environmental decision-making. Ecological Applications 6(4):1036 -1046.

Fogarty, M. J., M. P. Sissenwine, and E. B. Cohen. 1991. Recruitment variability and the dynamics of exploited marine populations. Trends in Ecology & Evolution 6(8):241-246.

Freckleton, R. P., A. R. Watkinson, R. E. Green, and W. J. Sutherland. 2006. Census error and the detection of density dependence. Journal of Animal Ecology 75(4):837-851.

Gelman, A. 2006. Prior distributions for variance parameters in hierarchical models. Bayesian Analysis:515-534.

Gelman, A., J. B. Carlin, H. S. Stern, and D. B. Rubin. 2014. Bayesian data analysis, volume 2. Chapman & Hall/CRC Boca Raton, FL, USA.

Gelman, A., and D. B. Rubin. 1992. Inference from iterative simulation using multiple sequences. Statistical Science 7(4):457-472.

Gleason, D., and G. M. Wellington. 1988. Food resources of postlarval brown shrimp (*Penaeus aztecus*) in a Texas salt marsh. Marine Biology 97(3):329-337.

Haas, H. L., E. C. Lamon I, K. A. Rose, and R. F. Shaw. 2001. Environmental and biological factors associated with the stage-specific abundance of brown shrimp (*Penaeus aztecus*) in Louisiana: applying a new combination of statistical techniques to long-term monitoring data. Canadian Journal of Fisheries & Aquatic Sciences 58(11):2258-2270.

Haas, H. L., K. A. Rose, B. Fry, T. J. Minello, and L. P. Rozas. 2004. Brown shrimp on the edge: linking habitat to survival using an individual-based simulation model. Ecological Applications 14(4):1232-1247.

Hart, R. A. 2012. Stock assessment of brown shrimp (*Farfantepenaeus aztecus*) in the U.S. Gulf of Mexico for 2011. NOAA Technical Memorandum NMFS-SEFSC-638:37.

Harvey, A. C. 1990. Forecasting, structural time series models and the Kalman filter. Cambridge University Press, New York, NY.

Hassell, M. 1975. Density-dependence in single-species populations. The Journal of Animal Ecology:283-295.

Hicks, S. D., H. A. J. Debaugh, and L. E. J. Hickman. 1983. Sea level variations for the United States, 1855-1980. National Ocean Survey, Rockville, MD (USA), NOAA-6901525.

Hilborn, R., and C. J. Walters. 2013. Quantitative fisheries stock assessment: choice, dynamics and uncertainty. Springer Science & Business Media.

Hixon, M. A. 1998. Population dynamics of coral-reef fishes: Controversial concepts and hypotheses. Austral Ecology 23(3):192-201.

Hjort, J. 1914. Fluctuations in the great fisheries of northern Europe viewed in the light of biological research. ICES.

Hobbs, N. T., and M. B. Hooten. 2015. Bayesian models: a statistical primer for ecologists. Princeton University Press.

Hooten, M. B., and N. Hobbs. 2015. A guide to Bayesian model selection for ecologists. Ecological Monographs 85(1):3-28.

Houde, E. D. 1987. Fish early life dynamics and recruitment variability. Pages 17-29 *in* American Fisheries Society Symposium.

Houde, E. D. 1989. Comparative growth, mortality, and energetics of marine fish larvae: temperature and implied latitudinal effects. Fishery Bulletin 87(3):471-495.

Houde, E. D. 1997. Patterns and consequences of selective processes in teleost early life histories. Pages 173-196 *in* R. C. Chambers, and E. A. Trippel, editors. Early Life History and Recruitment in Fish Populations. Springer Netherlands, Dordrecht.

Knape, J., and P. de Valpine. 2012. Are patterns of density dependence in the Global Population Dynamics Database driven by uncertainty about population abundance? Ecology Letters 15(1):17-23.

Kneib, R. 1995. Behaviour separates potential and realized effects of decapod crustaceans in salt marsh communities. Journal of Experimental Marine Biology and Ecology 193(1-2):239-256.

Kneib, R., and S. Wagner. 1994. Nekton use of vegetated marsh habitats at different stages of tidal inundation. Marine Ecology Progress Series 106(3):227-238.

Kneib, R. T. 1984. Patterns of invertebrate distribution and abundance in the intertidal salt marsh: Causes and questions. Estuaries 7(4):392-412.

Knudsen, P., W. Herke, and E. Knudsen. 1985. Emigration of brown shrimp from a low-salinity shallow-water marsh. Pages 30-40 *in* Proceedings of the Louisiana Academy of Science.

Kruschke, J. 2014. Doing Bayesian data analysis: A tutorial with R, JAGS, and Stan. Academic Press.

Lassuy, D. R. 1983. Species profiles - life histories and environmental requirements (Gulf of Mexico): brown shrimp. Fish and Wildlife Service, Slidell, LA (USA). National Coastal Ecosystems Team, FWS/OBS-82/11.1.

Lebreton, J. D., and O. Gimenez. 2013. Detecting and estimating density dependence in wildlife populations. The Journal of Wildlife Management 77(1):12-23.

Loesch, H. 1965. Distribution and growth of penaeid shrimp in Mobile Bay, Alabama. Publications of the Institute of Marine Science, University of Texas 10:41-58.

Mangel, M., and C. W. Clark. 1988. Dynamic modeling in behavioral ecology. Princeton University Press.

May, R. M. 1986. The search for patterns in the balance of nature: advances and retreats. Ecology 67(5):1115-1126.

McCoy, E. G. 1972. Dynamics of North Carolina commercial shrimp populations, volume 21. Division of Commercial and Sports Fisheries, North Carolina Department of Natural and Economic Resources.

McTigue, T. A., and R. J. Zimmerman. 1998. The use of infauna by juvenile *Penaeus aztecus* Ives and *Penaeus setiferus (*Linnaeus*)*. Estuaries 21(1):160-175.

Minello, T., and J. Webb Jr. 1997. Use of natural and created Spartina alterniflora salt marshes by fishery species and other aquatic fauna in Galveston Bay, Texas, USA. Marine Ecology Progress Series 151:165-179.

Minello, T. J., G. A. Matthews, P. A. Caldwell, and L. P. Rozas. 2008. Population and production estimates for decapod crustaceans in wetlands of Galveston Bay, Texas. Transactions of the American Fisheries Society 137(1):129-146.

Minello, T. J., and L. P. Rozas. 2002. Nekton in Gulf Coast wetlands: fine-scale distributions, landscape patterns, and restoration implications. Ecological Applications 12(2):441-455.

Minello, T. J., L. P. Rozas, and R. Baker. 2012. Geographic variability in salt marsh flooding patterns may affect nursery value for fishery species. Estuaries and Coasts 35(2):501-514.

Minello, T. J., L. P. Rozas, S. P. Hillen, and J. A. Salas. 2015. Variability in salt marsh flooding patterns in Galveston Bay, Texas. NOAA Technical Memorandum NMFS-SEFSC 678:12.

Minello, T. J., and R. Wooten Jr. 1993. Effects of caging juvenile predators on benthic infaunal populations at experimental open bay disposal areas in Galveston Bay, Texas. National Marine Fisheries Service, Southeast Fisheries Center.

Minello, T. J., and R. J. Zimmerman. 1983. Fish predation on juvenile brown shrimp, *Penaeus aztecus Ives*: The effect of simulated Spartina structure on predation rates. Journal of Experimental Marine Biology and Ecology 72(3):211-231.

Minello, T. J., and R. J. Zimmerman. 1991. The role of estuarine habitats in regulating growth and survival of juvenile penaeid shrimp. Frontiers in Shrimp Research:1-16.

Minello, T. J., R. J. Zimmerman, and E. X. Martinez. 1989. Mortality of young brown shrimp *Penaeus aztecus* in estuarine nurseries. Transactions of the American Fisheries Society 118(6):693-708.

Minello, T. J., R. J. Zimmerman, and R. Medina. 1994. The importance of edge for natant macrofauna in a created salt marsh. Wetlands 14(3):184-198.

Murdoch, W. W. 1994. Population regulation in theory and practice. Ecology 75(2):272-287.

Murray, B. G. 1994. On density dependence. Oikos:520-523.

Nance, J. M. 1989. Stock assessment for brown, white and pink shrimp in the US Gulf of Mexico, 1960-1987. US National Oceanic and Atmospheric Administration.

Nance, J. M. 2008. Stock Assessment Report 2007 Gulf of Mexico Shrimp Fishery. NMFS SEFSC Galveston Labratory.

Nance, J. M. 2014. Forecast for the 2014 brown shrimp season in the western Gulf of Mexico, from the Mississippi River to the U.S. - Mexico border. National Marine Fisheries Science Center Galveston Labratory.

Nance, J. M. 2015. Forecast for the 2015 brown shrimp season in the western Gulf of Mexico, from the Mississippi River to the U.S. - Mexico border. Southeast Fisheries Science Center Galveston Labratory.

Nance, J. M. 2016. Forecast for the 2016 brown shrimp season in the western Gulf of Mexico, from the Mississippi River to the U.S. - Mexico border. Southeast Fisheries Science Center, Galveston Labratory.

Nichols, S. 1984. Updated assessments of brown, white and pink shrimp in the US Gulf of Mexico. Workshop on Stock Assessment. Miami, Florida.

NOAA Fisheries Statistics. 2015. Commercial Fisheries Statistics, Annual Landings, http://www.st.nmfs.noaa.gov/commercial-fisheries/commercial-landings/annual-landings/index.

Pauly, D. 1980. On the interrelationships between natural mortality, growth parameters, and mean environmental temperature in 175 fish stocks. Journal du Conseil 39(2):175-192.

Pepin, P. 1991. Effect of temperature and size on development, mortality, and survival rates of the pelagic early life history stages of marine fish. Canadian Journal of Fisheries and Aquatic Sciences 48(3):503-518.

Plummer, M. 2003. JAGS: A program for analysis of Bayesian graphical models using Gibbs sampling. Pages 20-22 *in* 3rd Distributed Statistical Computing 2003.

Plummer, M. 2008. Penalized loss functions for Bayesian model comparison. Biostatistics 9(3):523-539.

R Core Team. 2015. R: A language and environment for statistical computing R Foundation for Statistical Computing Vienna, Austria

Rader, D. N. 1984. Salt-marsh benthic invertebrates: small-scale patterns of distribution and abundance. Estuaries 7(4):413-420.

Ray, C., and A. Hastings. 1996. Density dependence: are we searching at the wrong spatial scale? Journal of Animal Ecology 65(5):556-566.

Riera, P., P. Montagna, R. Kalke, and P. Richard. 2000. Utilization of estuarine organic matter during growth and migration by juvenile brown shrimp *Penaeus aztecus* in a south Texas estuary. Marine Ecology Progress Series 199:205-216.

Rivot, E., E. Prévost, E. Parent, and J. L. Baglinière. 2004. A Bayesian state-space modelling framework for fitting a salmon stage-structured population dynamic model to multiple time series of field data. Ecological Modelling 179(4):463-485.

Rosas, C., L. Ocampo, G. Gaxiola, A. Sánchez, and L. A. Soto. 1999. Effect of salinity on survival, growth, and oxygen consumption of postlarvae (PL10-PL21) of *Litopenaeus setiferus*. Journal Crustacean Biology:244-251.

Rose, K. A., J. H. Cowan, K. O. Winemiller, R. A. Myers, and R. Hilborn. 2001. Compensatory density dependence in fish populations: importance, controversy, understanding and prognosis. Fish and Fisheries 2(4):293-327.

Roth, B., K. Rose, L. Rozas, and T. Minello. 2008. Relative influence of habitat fragmentation and inundation on brown shrimp *Farfantepenaeus aztecus* production in northern Gulf of Mexico salt marshes. Marine Ecological Progress Series 359:185.

Rozas, L. P. 1995. Hydroperiod and its influence on nekton use of the salt marsh: A pulsing ecosystem. Estuaries 18(4):579-590.

Rozas, L. P., and T. J. Minello. 2009. Using nekton growth as a metric for assessing habitat restoration by marsh terracing. Marine Ecology Progress Series 394:179-193.

Rozas, L. P., and T. J. Minello. 2011. Variation in penaeid shrimp growth rates along an estuarine salinity gradient: implications for managing river diversions. Journal of Experimental Marine Biology and Ecology 397(2):196-207.

Rozas, L. P., T. J. Minello, R. J. Zimmerman, and P. Caldwell. 2007. Nekton populations, long-term wetland loss, and the effect of recent habitat restoration in Galveston Bay, Texas, USA. Marine Ecological Progress Series 344:119-130.

Rozas, L. P., and W. E. Odum. 1988. Occupation of submerged aquatic vegetation by fishes: testing the roles of food and refuge. Oecologia 77(1):101-106.

Rozas, L. P., and D. J. Reed. 1994. Comparing nekton assemblages of subtidal habitats in pipeline canals traversing brackish and saline marshes in coastal Louisiana. Wetlands 14(4):262-275.

Rozas, L. P., and R. J. Zimmerman. 2000. Small-scale patterns of nekton use among marsh and adjacent shallow nonvegetated areas of the Galveston Bay Estuary, Texas (USA). Marine Ecological Progress Series 193:217-239.

Saoud, I. P., and D. A. Davis. 2003. Salinity tolerance of brown shrimp *Farfantepenaeus aztecus* as it relates to postlarval and juvenile survival, distribution, and growth in estuaries. Estuaries 26(4):970-974.

Scavia, D., and coauthors. 2002. Climate change impacts on US coastal and marine ecosystems. Estuaries 25(2):149-164.

Shepherd, J. G., and D. H. Cushing. 1980. A mechanism for density-dependent survival of larval fish as the basis of a stock-recruitment relationship. ICES Journal of Marine Science 39(2):160-167.

Shepherd, J. G., D. H. Cushing, and R. J. H. Beverton. 1990. Regulation in fish populations: myth or mirage? Philosophical Transactions of the Royal Society of London. Series B: Biological Sciences 330(1257):151-164.

Simpson, E. H. 1951. The interpretation of interaction in contingency tables. Journal of the Royal Statistical Society. Series B (Methodological) 13(2):238-241.

Sinclair, A. R. E., and R. P. Pech. 1996. Density dependence, stochasticity, compensation and predator regulation. Oikos 75(2):164-173.

Sissenwine, M. P. 1984. Why do fish populations vary? Pages 59-94 *in* R. M. May, editor. Exploitation of Marine Communities. Springer Berlin Heidelberg, Berlin, Heidelberg.

Sogard, S. M. 1997. Size-selective mortality in the juvenile stage of teleost fishes: a review. Bulletin of Marine Science 60(3):1129-1157.

Spiegelhalter, D. J., N. G. Best, B. P. Carlin, and A. Van Der Linde. 2002. Bayesian measures of model complexity and fit. Journal of the Royal Statistical Society: Series B (Statistical Methodology) 64(4):583-639.

St Amant, L., K. Corkum, and J. Broom. 1963. Studies on growth dynamics of the brown shrimp, Penaeus aztecus. Louisiana waters. Ann. Session Gulf Caribb. Fish. Inst. Proc. 15:14-26.

Turchin, P. 1999. Population regulation: A synthetic view. Oikos 84(1):153-159.

Turner, R. E. 1991. Tide gauge records, water level rise, and subsidence in the Northern Gulf of Mexico. Estuaries 14(2):139-147.

Voorhees, D. V. 2011. Fisheries of the United States. National Marine Fisheries Service, Silver Spring, MD.

Ware, D. M. 1975. Relation between egg size, growth, and natural mortality of larval fish. Journal of the Fisheries Research Board of Canada 32(12):2503-2512.

Wenner, E. L., and H. R. Beatty. 1993. Utilization of shallow estuarine habitats in South Carolina, USA, by postlarval and juvenile stages of *Penaeus* spp. (Decapoda: Penaeidae). Journal of Crustacean Biology:280-295.

Werner, E. E., and J. F. Gilliam. 1984. The ontogenetic niche and species interactions in size-structured populations. Annual Review of Ecology and Systematics 15:393-425.

Whaley, S. D. 1997. The effects of marsh edge and surface elevation on the distribution of salt marsh infauna and prey availability for nekton predators. Texas A&M University.

Whaley, S. D., and T. J. Minello. 2002. The distribution of benthic infauna of a Texas salt marsh in relation to the marsh edge. Wetlands 22(4):753-766.

Williams, A. B. 1955. A contribution to the life histories of commercial shrimps (*Penaeidae*) in North Carolina. Bulletin of Marine Science 5(2):116-146.

Zein-Eldin, Z. P., and D. V. Aldrich. 1965. Growth and survival of postlarval *Penaeus aztecus* under controlled conditions of temperature and salinity. The Biological Bulletin 129(1):199-216.

Zein-Eldin, Z. P., and G. W. Griffith. 1966. The effect of temperature upon the growth of laboratory-held postlarval *Penaeus aztecus*. The Biological Bulletin 131(1):186-196.

Zein-Eldin, Z. P., and G. W. Griffith. 1967. An appraisal of the effects of salinity and temperature on growth and survival of postlarval penaeids. Bureau of Commercial Fisheries.

Zein-Eldin, Z. P., and M. L. Renaud. 1986. Inshore environmental effects on brown shrimp, *Penaeus aztecus*, and white shrimp, *P. setiferus*, populations in coastal waters, particularly of Texas. Marine Fisheries Review 48(3):9-19.

Zimmerman, R. J., and T. J. Minello. 1984. Densities of *Penaeus aztecus*, *Penaeus setiferus*, and other natant macrofauna in a Texas salt marsh. Estuaries and Coasts 7(4):421-433.

Zimmerman, R. J., T. J. Minello, M. Castiglione, and D. Smith. 1990. Utilization of marsh and associated habitats along a salinity gradient in Galveston Bay. US Dept. of Commerce, National Oceanic and Atmospheric Administration, National Marine Fisheries Service, Southeast Fisheries Center, Galveston Laboratory.

Zimmerman, R. J., T. J. Minello, E. F. Klima, and J. M. Nance. 1991. Effects of accelerated sea-level rise on coastal secondary production. American Society of Civil Engineers.

Zimmerman, R. J., T. J. Minello, and G. Zamora. 1984. Selection of vegetated habitat by brown shrimp, *Penaeus aztecus*, in a Galveston Bay salt marsh. Fishery Bulletin 82(2):325-336.

# APPENDIX A
# CONVERGENCE DIAGNOSTICS

Convergence was determined based on the potential scale reduction factor (psrf) a Gelman-Rubin statistic, and visual inspection of the trace plot and density plot for each parameter. Visual inspection of a trace plot (top left panel) with overlapping chains and a band that is relatively level indicates convergence (Hobbs and Hooten 2015; Kruschke 2014). Density plots (bottom right panel) that overlap imply the chains provide a good posterior distribution (Kruschke 2014).

The Monte Carlo standard error (MCSE), autocorrelation plot and value and effective sample size (ESS) were used to determine the stability and accuracy of the HDI and parameter estimates. The Monte Carlo Standard Error ($\text{MCSE} = \frac{\text{SD}}{\sqrt{\text{ESS}}}$) indicates the standard error of the mean of the posterior distribution, or the accuracy of the posterior distribution, on the scale of the parameter (Kruschke 2014). The autocorrelation plot (top right panel) is a visual representation of the amount of dependence of one sample on the previous sample (Hobbs and Hooten 2015). A low autocorrelation value indicates a well-mixed chain that has explored the posterior sufficiently. Very high autocorrelation indicates successive steps in the chain may not be independent and could indicate a parameter is not identifiable (Hobbs and Hooten 2015; Kruschke 2014). The effective sample size (ESS) ($\text{ESS} = \frac{\text{actual sample size}}{\text{amount of autocorrelation}}$) is a measure of how well the posterior distribution has been sampled (Hobbs and Hooten 2015; Kruschke 2014). When the limits of the HDI are of interest, Kruschke (2014) recommends a high ESS (10,000) to ensure the less sampled margins of the distribution are sufficiently sampled. For statistics that are more influenced by dense regions of an HDI, such as the median, a lower ESS is allowable, although Kruschke (2014) does not recommend an $\text{ESS} \leq 100$.

Table A-1: Size-dependent survival (SDS) model convergence diagnostics.

| **Parameter** | **Monte Carlo standard error (MSCE)** | **Effective sample size (ESS)** | **Gelman-Rubin statistics (psrf)** |
|---|---|---|---|
| z1 | 0.000148 | 149648.7 | 1.0001 |
| z2 | 0.00011 | 294292 | 1.0003 |
| z3 | 0.000113 | 373144.4 | 1 |
| z4 | 0.000162 | 459780.5 | 1 |
| p1 | 0.000272 | 130052.7 | 1.0002 |
| p2 | 0.000196 | 202747.2 | 1.0001 |
| $\tau^2$ | 0.00149 | 4582.6 | 1.0034 |
| $\sigma^2$ | 0.00188 | 7678.6 | 1.0027 |

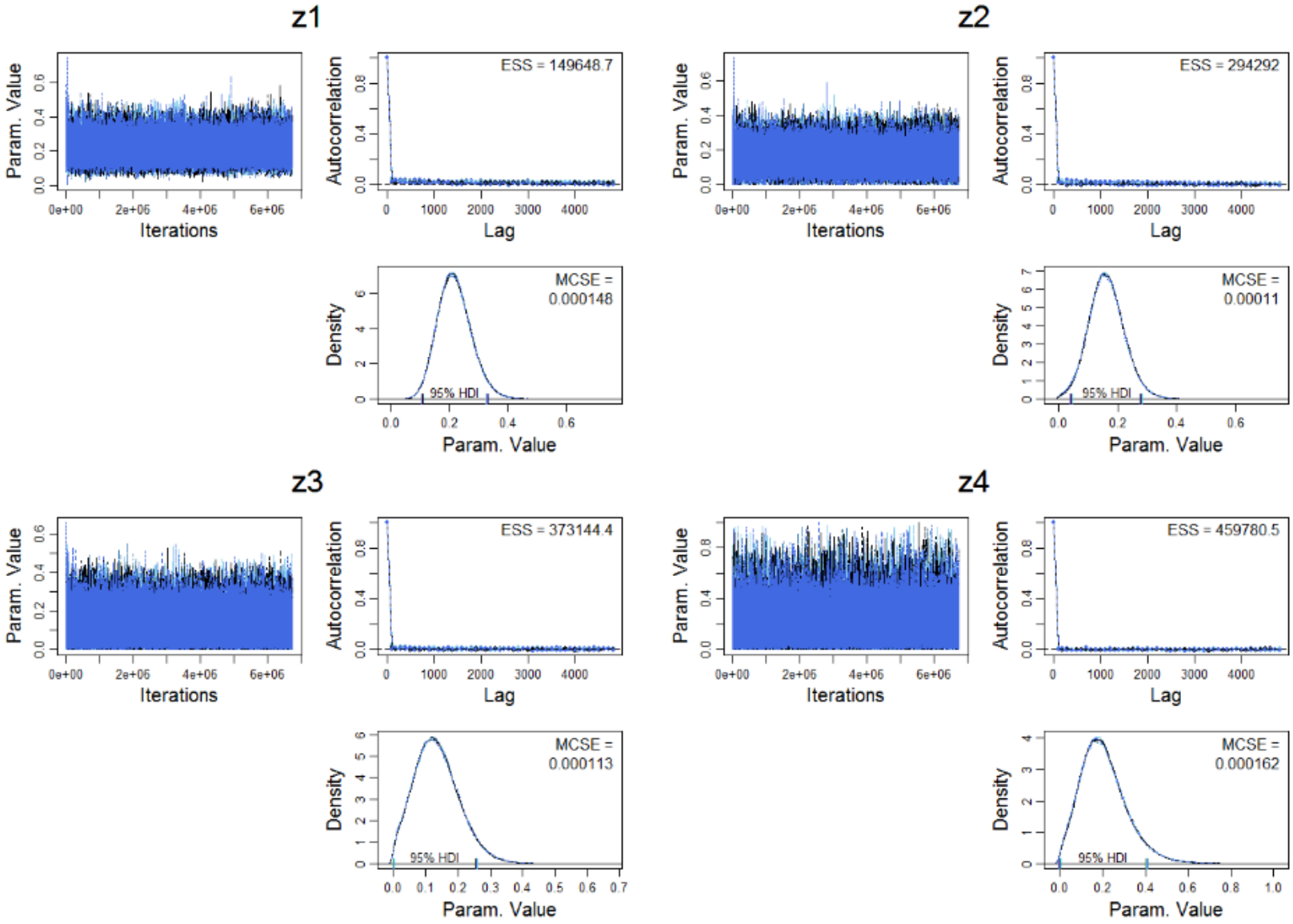


Figure A-1: Size-dependent survival (SDS) model convergence diagnostics. Figures for each parameter include a trace plot (top left), autocorrelation plot with effective sample size (ESS) (top right) and a density plot with Monte Carlo Standard error (MCSE) (bottom right).

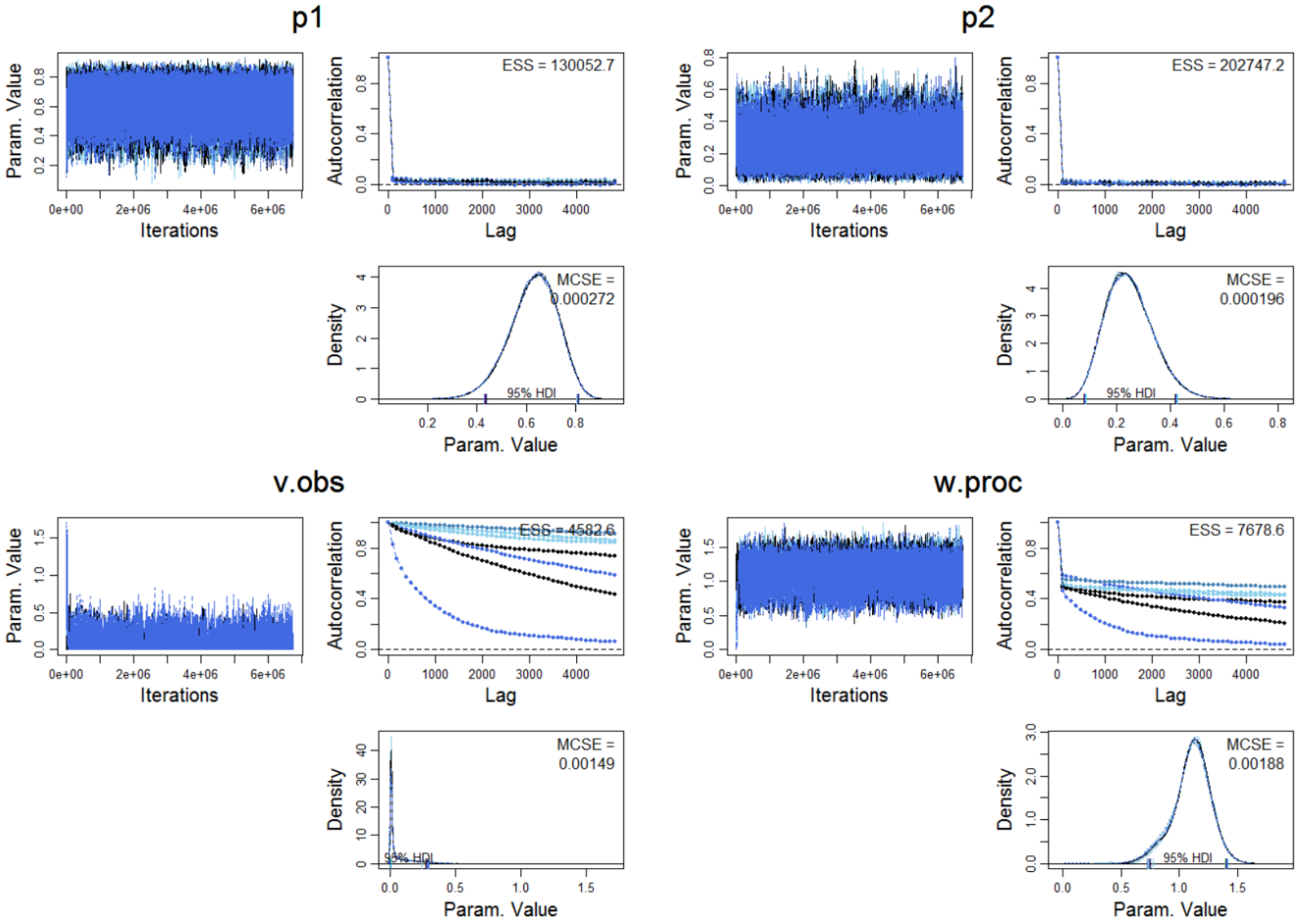


Figure A-1 continued.

Table A-2: Within stage density-dependent survival (BW) model convergence diagnostics.

| **Parameter** | **Monte Carlo standard error (MSCE)** | **Effective sample size (ESS)** | **Gelman-Rubin statistics (psrf)** |
|---|---|---|---|
| $\alpha$ | 0.000333 | 14111.1 | 1.0011 |
| $\beta$ | 2.25E-06 | 22482 | 1.0003 |
| p1 | 0.000286 | 124019.1 | 1.0002 |
| p2 | 0.00084 | 13200.2 | 1.0001 |
| $\tau^2$ | 0.0165 | 687.8 | 1.0032 |
| $\sigma^2$ | 0.00123 | 17771.3 | 1.0038 |

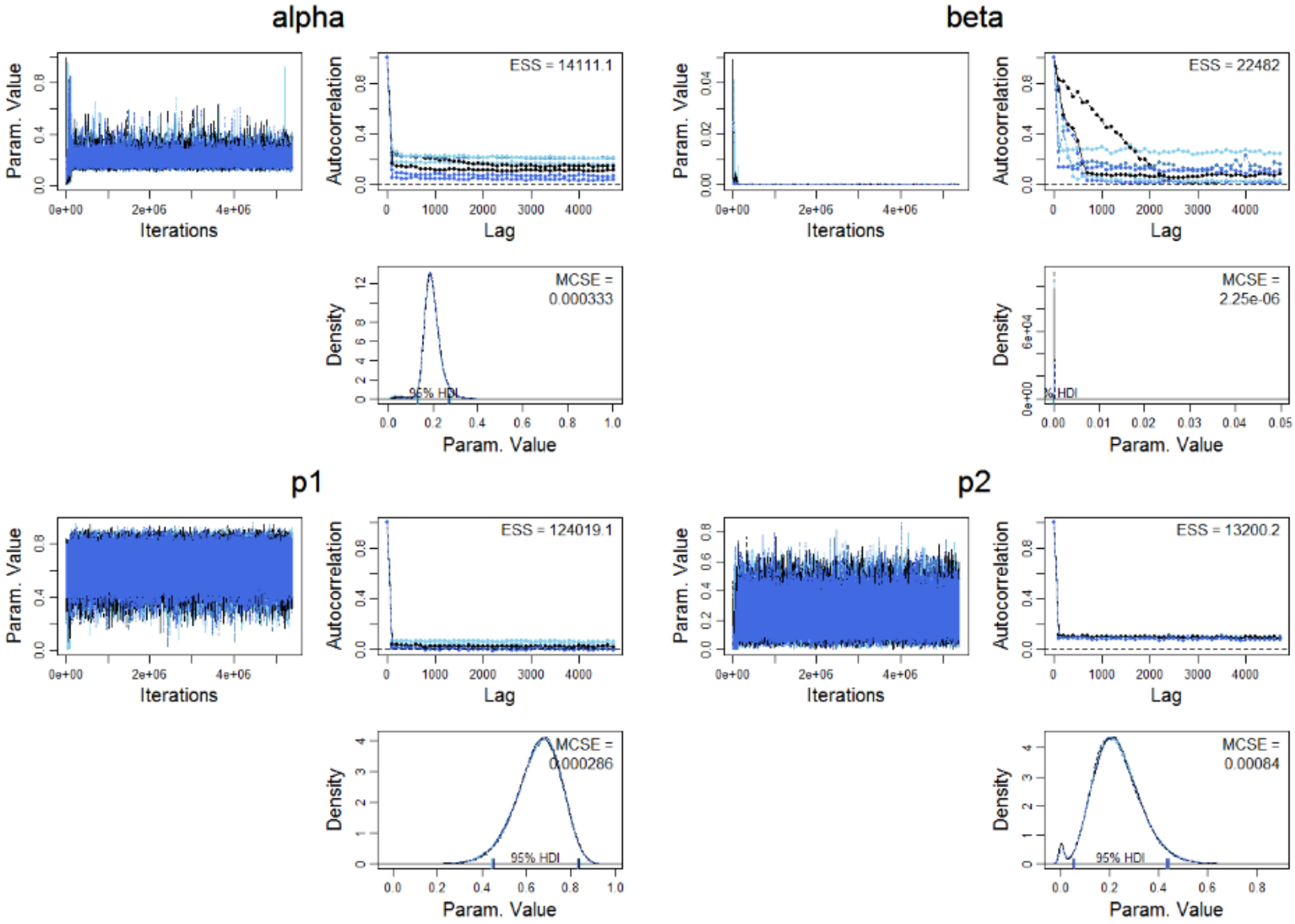


Figure A-2: Within stage density-dependent survival (BW) model convergence diagnostics. Figures for each parameter include a trace plot (top left), autocorrelation plot with effective sample size (ESS) (top right) and a density plot with Monte Carlo Standard error (MCSE) (bottom right).

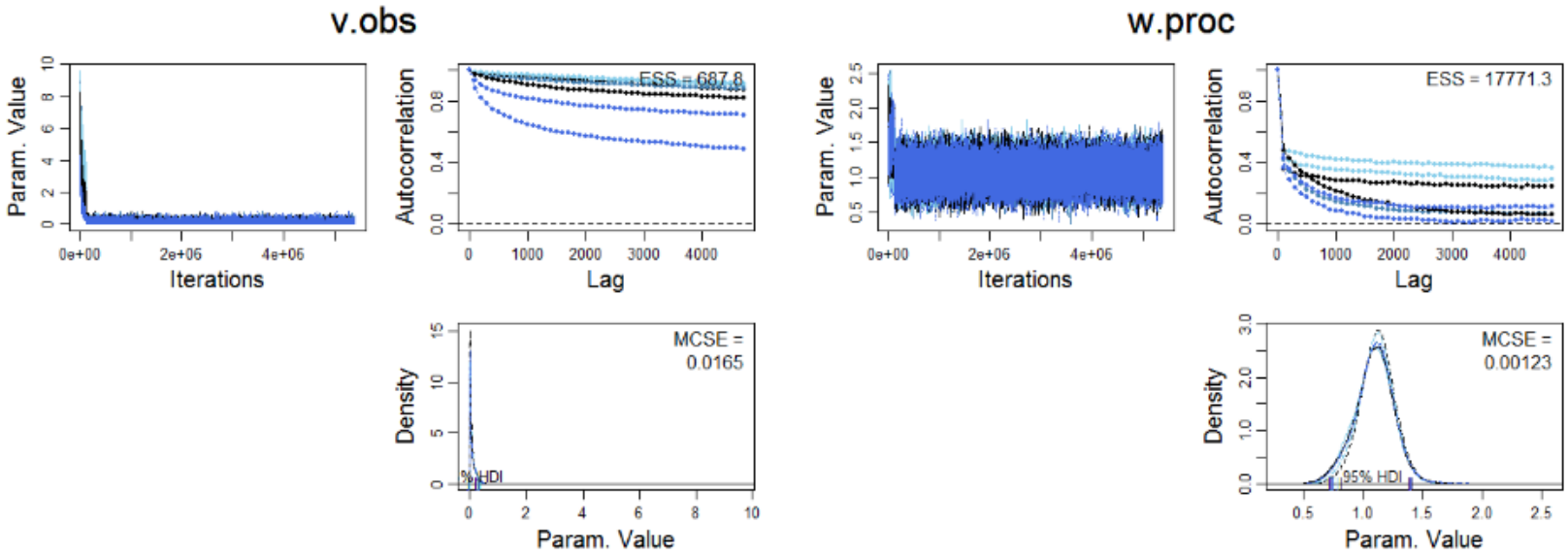


Figure A-2 continued.

Table A-3: Between all stage density-dependent survival (BA) model convergence diagnostics.

| **Parameter** | **Monte Carlo standard error (MSCE)** | **Effective sample size (ESS)** | **Gelman-Rubin statistics (psrf)** |
|---|---|---|---|
| $\alpha$ | 0.0101 | 130.5 | 1.0007 |
| $\beta$ | 0.000625 | 232.4 | 1.001 |
| p1 | 0.00494 | 582.8 | 1.0005 |
| p2 | 0.00266 | 1412.9 | 1.0007 |
| $\tau^2$ | 0.209 | 86.8 | 1.0004 |
| $\sigma^2$ | 0.185 | 84.3 | 1.0001 |

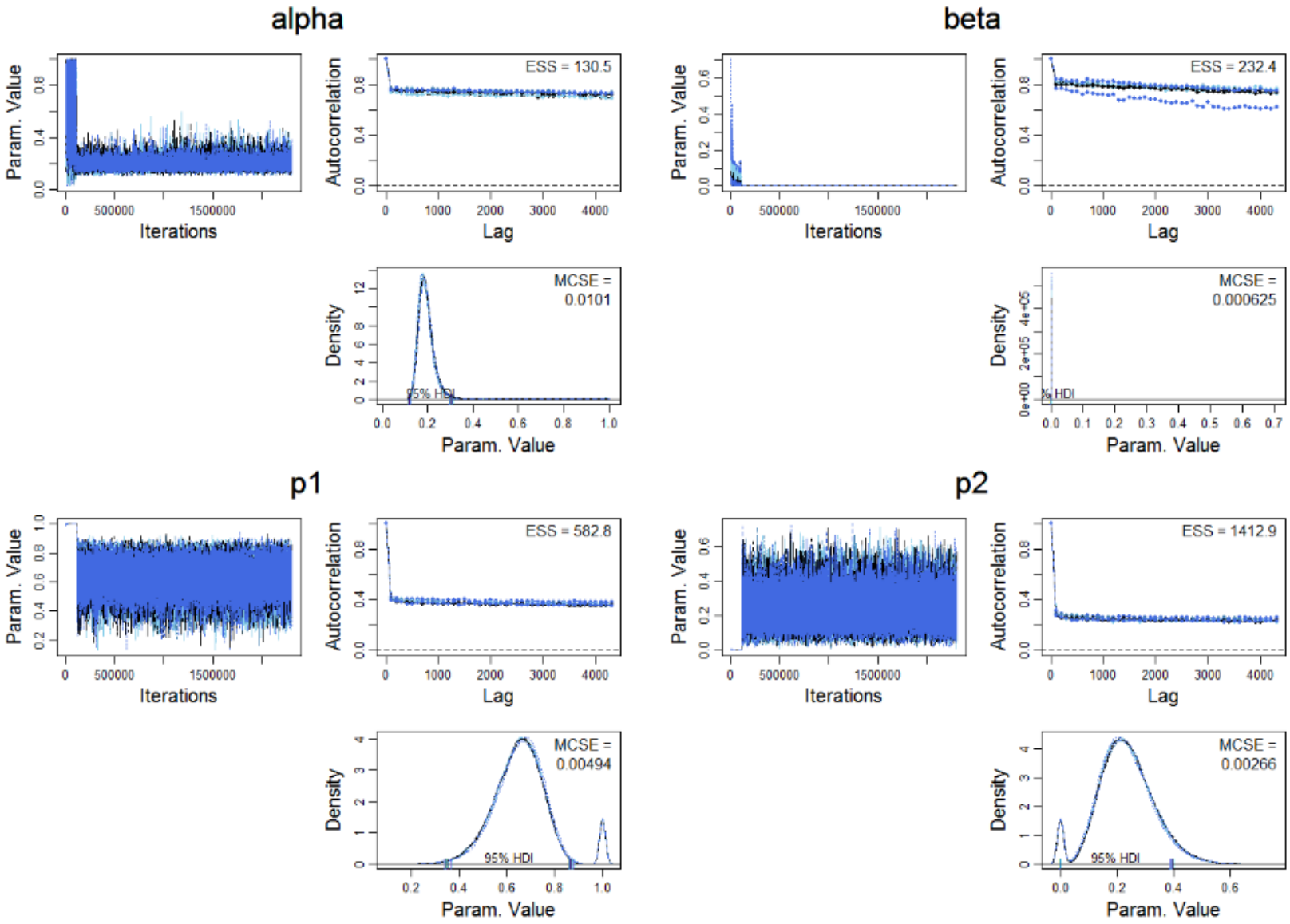


Figure A-3: Between all stages density-dependent survival (BA) model convergence diagnostics. Figures for each parameter include a trace plot (top left), autocorrelation plot with effective sample size (ESS) (top right) and a density plot with Monte Carlo Standard error (MCSE) (bottom right).

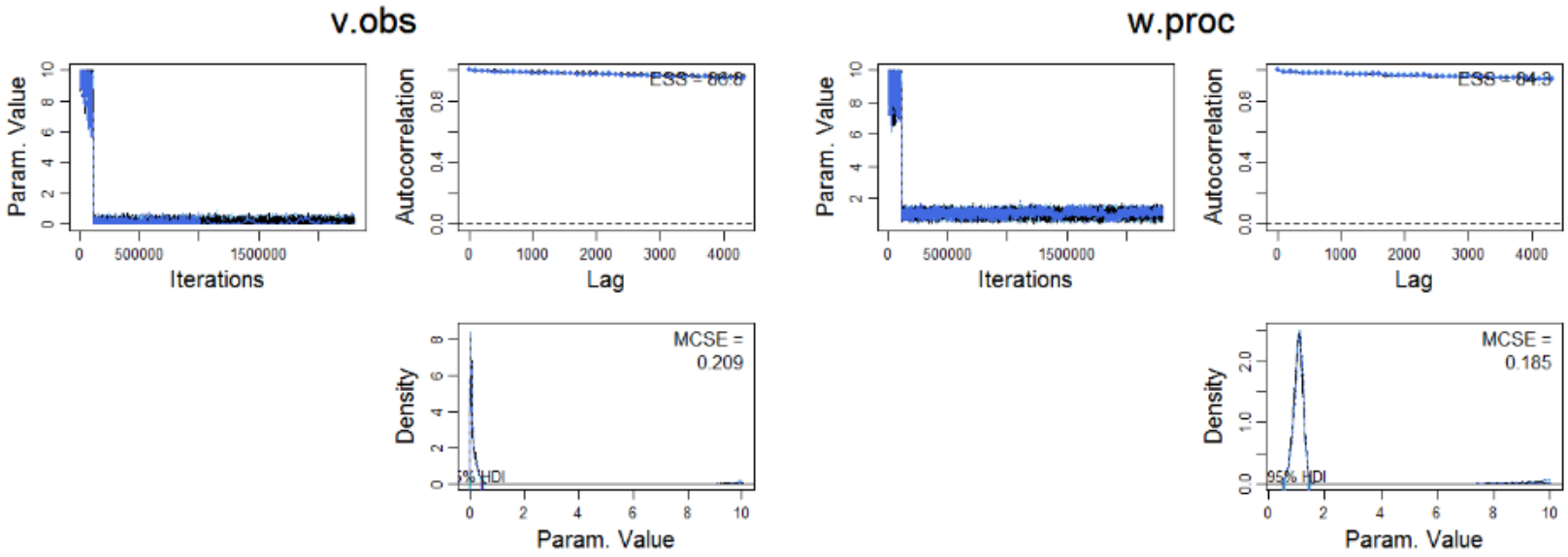


Figure A-3 continued.

Table A-4: Density and size-independent (NULL) model convergence diagnostics.

| **Parameter** | **Monte Carlo standard error (MSCE)** | **Effective sample size (ESS)** | **Gelman-Rubin statistics (psrf)** |
|---|---|---|---|
| z | 3.3E-05 | 422070 | 1 |
| p1 | 0.000188 | 265779.2 | 1 |
| p2 | 0.000163 | 301820.9 | 1 |
| $\tau^2$ | 0.000957 | 19204.9 | 1.0004 |
| $\sigma^2$ | 0.00108 | 27518.3 | 1.0016 |

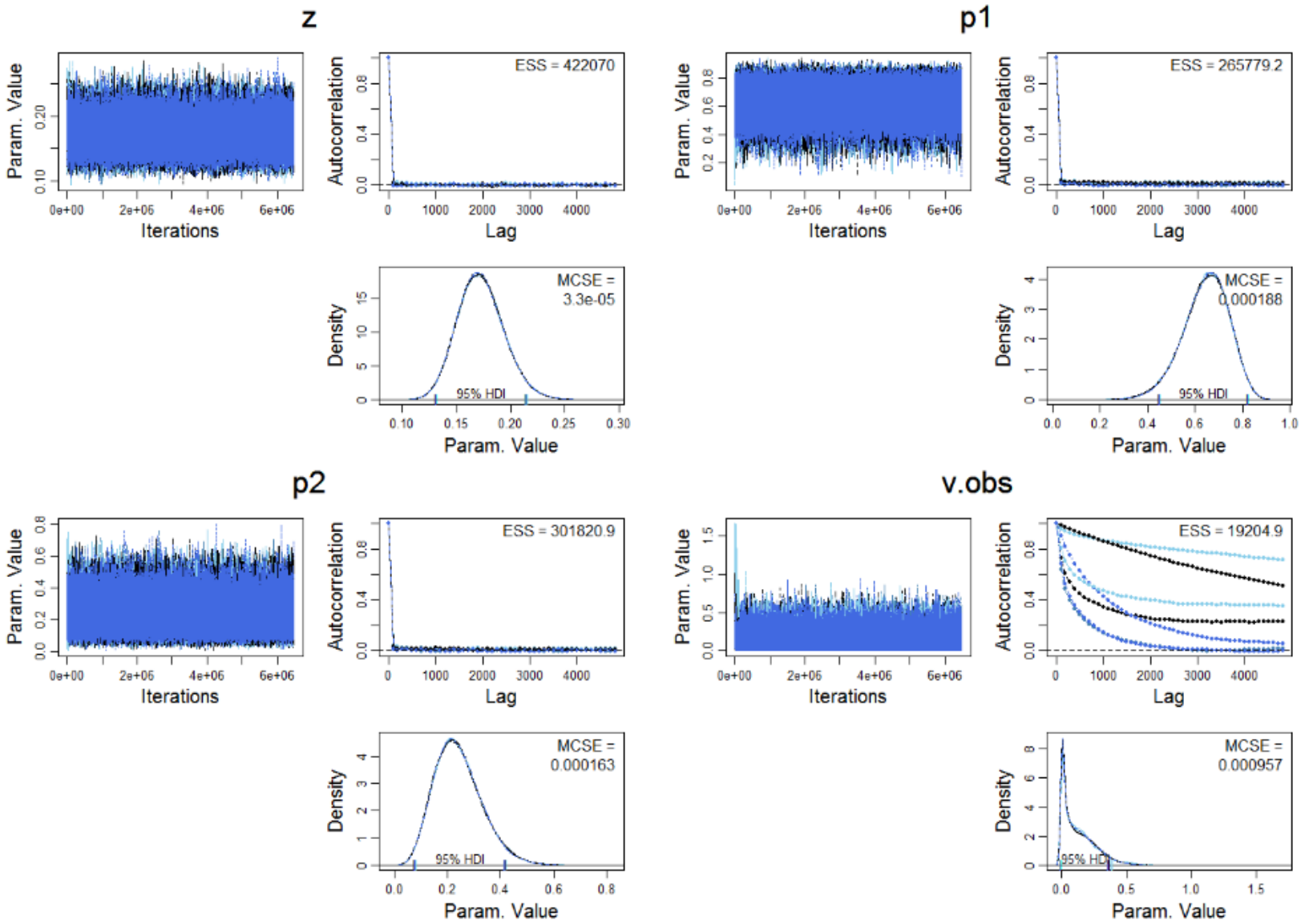


Figure A-4: Density and size-independent (NULL) model convergence diagnostics. Figures for each parameter include a trace plot (top left), autocorrelation plot with effective sample size (ESS) (top right) and a density plot with Monte Carlo Standard error (MCSE) (bottom right).

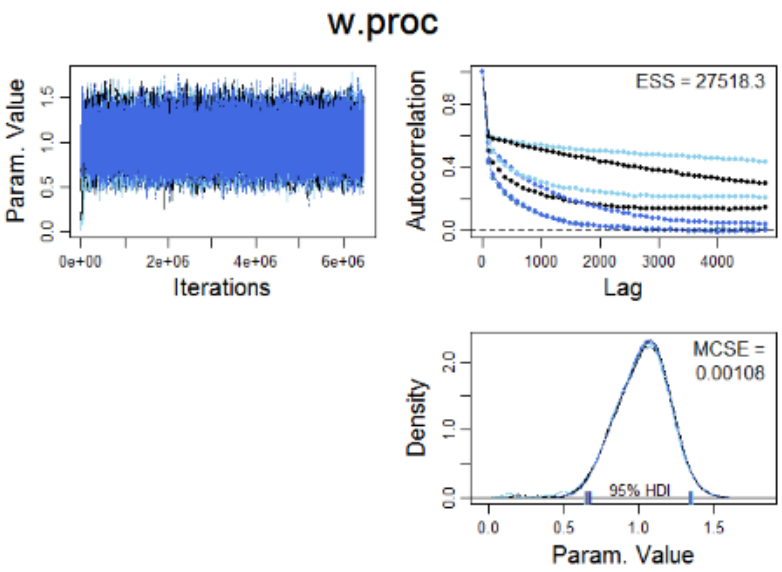


Figure A-4 continued

Table A-5: Size-dependent growth (SDG) model convergence diagnostics.

| **Parameter** | **Monte Carlo standard error (MSCE)** | **Effective sample size (ESS)** | **Gelman-Rubin statistics (psrf)** |
|---|---|---|---|
| z | 4.86E-05 | 376802.3 | 1 |
| p31 | 0.000171 | 435121.5 | 0.99998 |
| p42 | 2E-04 | 409640.2 | 1 |
| p53 | 0.000293 | 386875.7 | 1 |
| p64 | 0.000272 | 450067.5 | 0.99999 |
| p41 | 0.000139 | 461486.4 | 0.99999 |
| p52 | 0.000188 | 433358.1 | 1 |
| p63 | 0.00015 | 430550.4 | 1.0001 |
| $\tau^2$ | 0.00068 | 36266.1 | 1.0021 |
| $\sigma^2$ | 0.000838 | 45608.7 | 1.0008 |

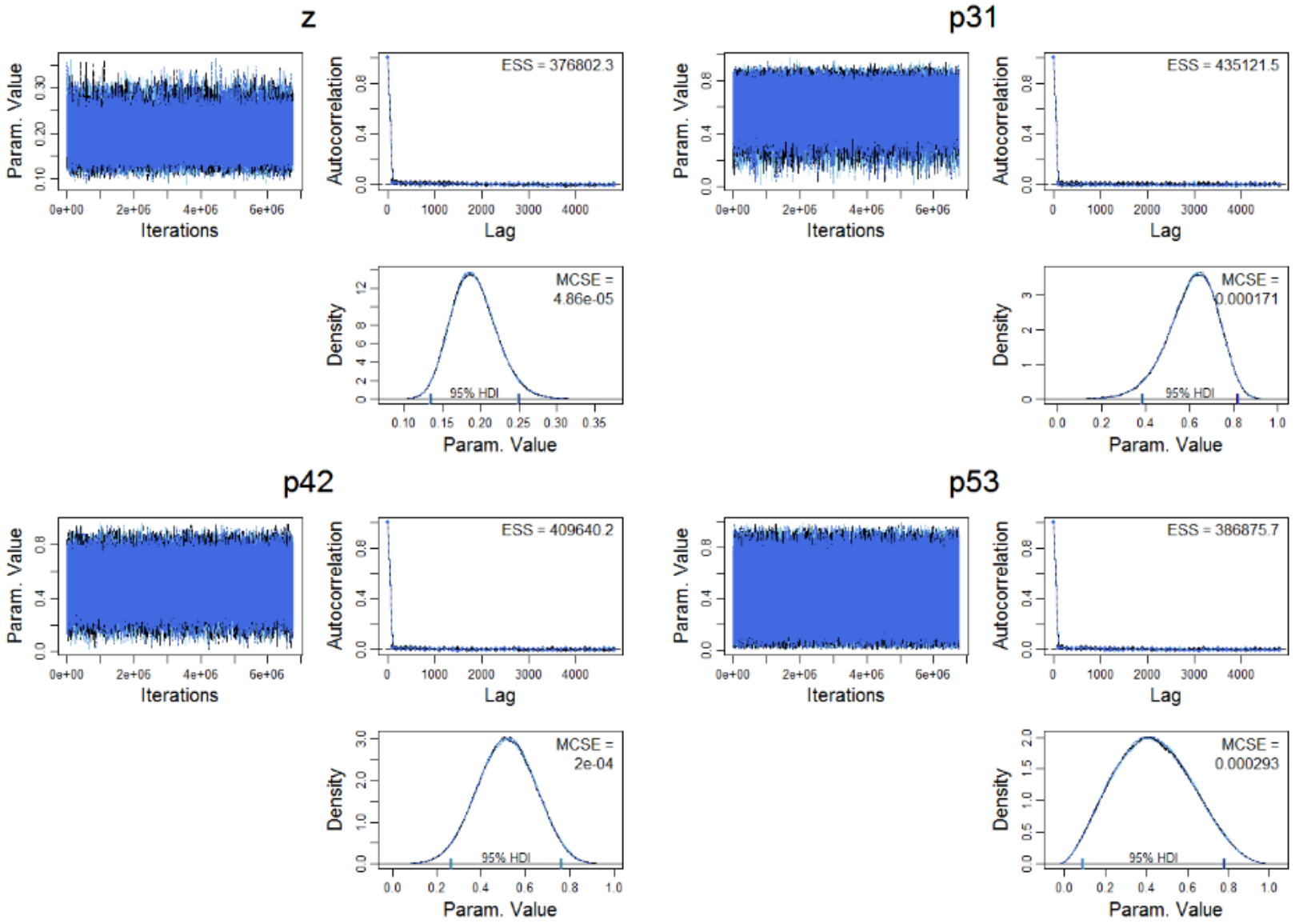


Figure A-5: Size-dependent growth (SDG) model convergence diagnostics. Figures for each parameter include a trace plot (top left), autocorrelation plot with effective sample size (ESS) (top right) and a density plot with Monte Carlo Standard error (MCSE) (bottom right).

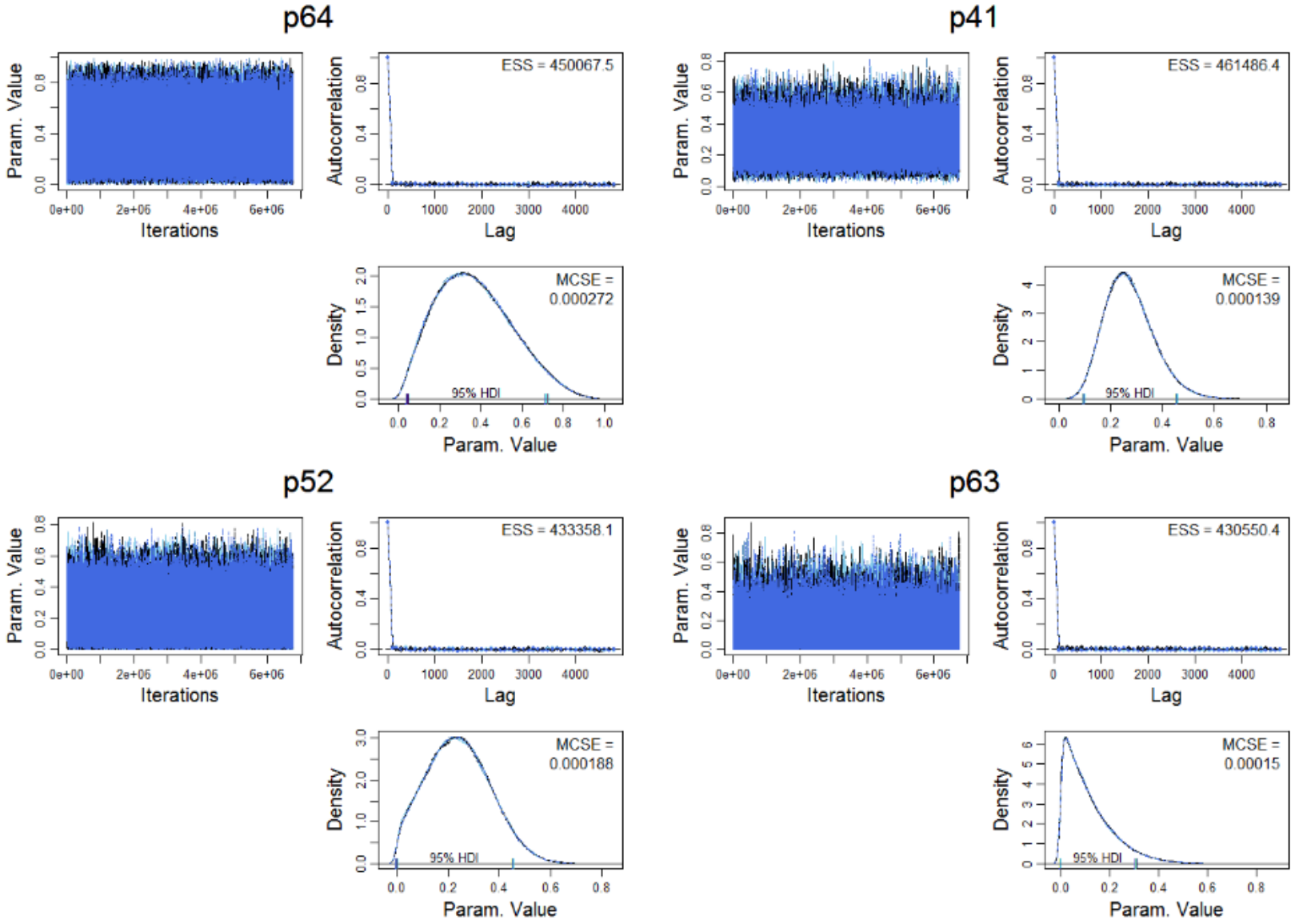


Figure A-5 continued.

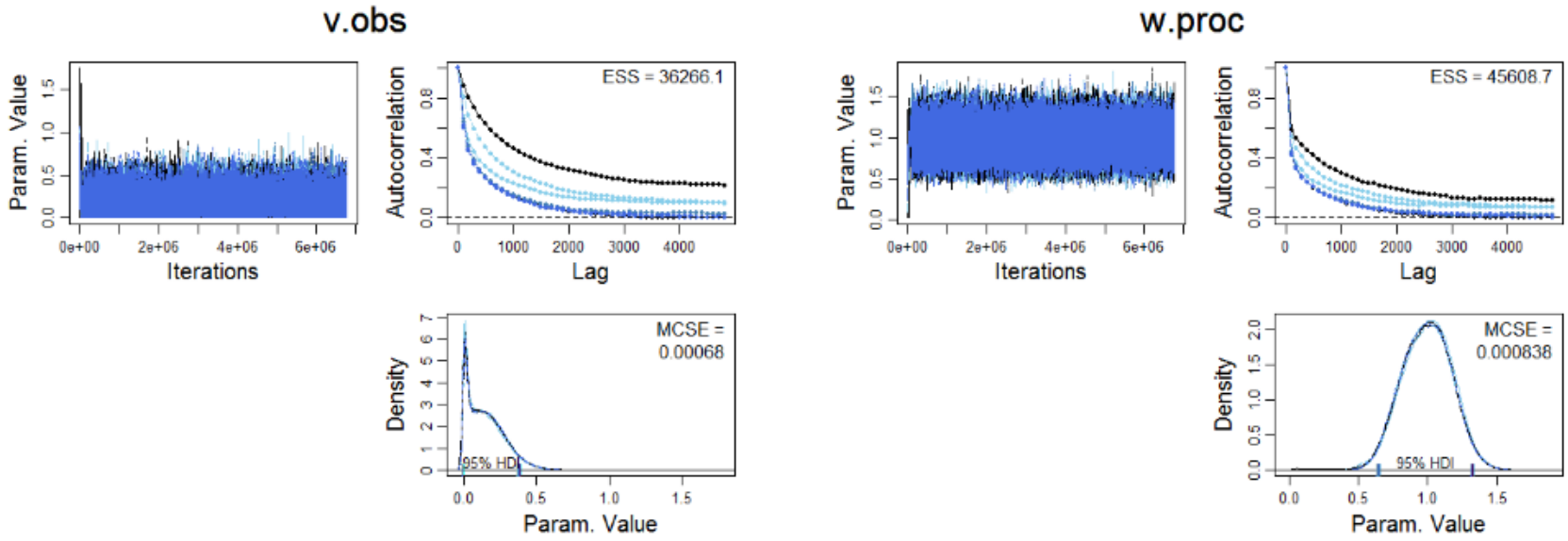


Figure A-5 continued.

# APPENDIX B

# PARAMETER 95% HIGHEST DENSITY INTERVALS AND STATISTICS

Posterior distributions are provided for each parameter in all models (see tables B-1 and B-2 and figures B-1 through B-5) with median and 95% highest density interval (HDI) reported. The 95% HDI, which indicates the most probable values in the posterior distribution with a total probability of 95%, is marked with a black bar in each figure. The width of the HDI indicates uncertainty, with a wider HDI indicating more uncertainty and a narrower indicating relatively more certainty about the parameters estimates (Kruschke 2014).

Table B-1: The median and 95% highest density interval (HDI) for process error variance ($\tau^2$), observation error variance ($\sigma^2$) and survival. In density-independent models (SDS, NULL, SDG) survival ($\varphi_i$) estimates the probability of survival in stage i, while survival in density-dependent models (BW, BA) estimates $\alpha_1$, maximum survival rate of at low densities, and $\beta_1$, strength of density-dependent mortality. Models ranked according to deviance information criterion (DIC). Models are in order of fit, with the best fit model reported in the first column of this table.

| **Model** | **Survival** | | | | **Error** | |
|---|---|---|---|---|---|---|
| **SDS** | $\boldsymbol{\varphi_1}$ | $\boldsymbol{\varphi_2}$ | $\boldsymbol{\varphi_3}$ | $\boldsymbol{\varphi_4}$ | **V.Obs ($\tau^2$)** | **W.Proc ($\sigma^2$)** |
| | 0.215 (0.110, 0.332) | 0.160 (0.046, 0.282) | 0.129 (0.0006, 0.258) | 0.193 (0.005, 0.409) | 0.00898 (0.001, 0.281) | 1.119 (0.746, 1.4) |
| **BW** | $\boldsymbol{\alpha_1}$ | | $\boldsymbol{\beta_1}$ | | 0.0384 (0.001, 0.328) | 1.11 (0.753, 1.41) |
| | 0.193 (0.135, 0.277) | | 1.74E-05 (3.19E-11, 8.00E-05) | | | |
| **BA** | $\boldsymbol{\alpha_1}$ | | $\boldsymbol{\beta_1}$ | | 0.056 (0.001, 0.480) | 1.09 (0.606, 1.5) |
| | 0.189 (0.122, 0.306) | | 4.77E-06 (1.37E-11, 3.85E-05) | | | |
| **NULL** | $\boldsymbol{\varphi}$ | | | | 0.0919 (0.001, 0.374) | 1.03 (0.668, 1.35) |
| | 0.171 (0.131, 0.215) | | | | | |
| **SDG** | $\boldsymbol{\varphi}$ | | | | 0.13 (0.001, 0.386) | 0.995 (0.648, 1.33) |
| | 0.189 (0.134, 0.25) | | | | | |

Table B-2: Median and 95% highest density interval (HDI) for growth ($\gamma_i$) for all models. The probability of growing 41 or more mm $\boldsymbol{\gamma_3 = 1 - \gamma_1 - \gamma_2}$. Rates in gray are confounded with emigration and may not be valid parameter estimates. Models ranked according to deviance information criterion (DIC) and parameter estimates reported as the median and 95% highest density interval (HDI). Models are in order of fit, with the best fit model reported in the first column of this table.

| **Model** | **Growth** | | | | | | | | | |
|---|---|---|---|---|---|---|---|---|---|---|
| **SDS** | **$\gamma_1$ = grow 20-30 mm** | | | | **$\gamma_2 = grow\ 31-40\ mm$** | | | $\gamma_3 = grow\ 41+mm$ | | |
| | 0.636 (0.433, 0.811) | | | | 0.240 (0.087, 0.425) | | | 0.124 | | |
| **BW** | **$\gamma_1$ = grow 20-30 mm** | | | | **$\gamma_2 = grow\ 31-40\ mm$** | | | $\gamma_3 = grow\ 41+mm$ | | |
| | 0.662 (0.453, 0.838) | | | | 0.220 (0.054, 0.435) | | | 0.118 | | |
| **BA** | **$\gamma_1$ = grow 20-30 mm** | | | | **$\gamma_2 = grow\ 31-40\ mm$** | | | $\gamma_3 = grow\ 41+mm$ | | |
| | 0.659 (0.355, 0.872) | | | | 0.224 (0.251E-09, 0.397) | | | 0.117 | | |
| **NULL** | **$\gamma_1$ = grow 20-30 mm** | | | | **$\gamma_2 = grow\ 31-40\ mm$** | | | $\gamma_3 = grow\ 41+mm$ | | |
| | 0.652 (0.45, 0.824) | | | | 0.232 (0.0764, 0.417) | | | 0.116 | | |
| **SDG** | $\boldsymbol{\gamma_{31}}$ | $\boldsymbol{\gamma_{42}}$ | $\boldsymbol{\gamma_{53}}$ | $\gamma_{64}$ | $\boldsymbol{\gamma_{41}}$ | $\boldsymbol{\gamma_{52}}$ | $\gamma_{63}$ | $\boldsymbol{\gamma_{51}}$ | $\gamma_{62}$ | $\gamma_{73}$ |
| | 0.622 (0.384, 0.819) | 0.515 (0.267, 0.765) | 0.427 (0.0948, 0.782) | 0.355 (0.0446, 0.72) | 0.262 (0.0978, 0.457) | 0.236 (0.00138, 0.455) | 0.0883 (1.92e-06, 0.312) | 0.116 | 0.249 | 0.4847 |

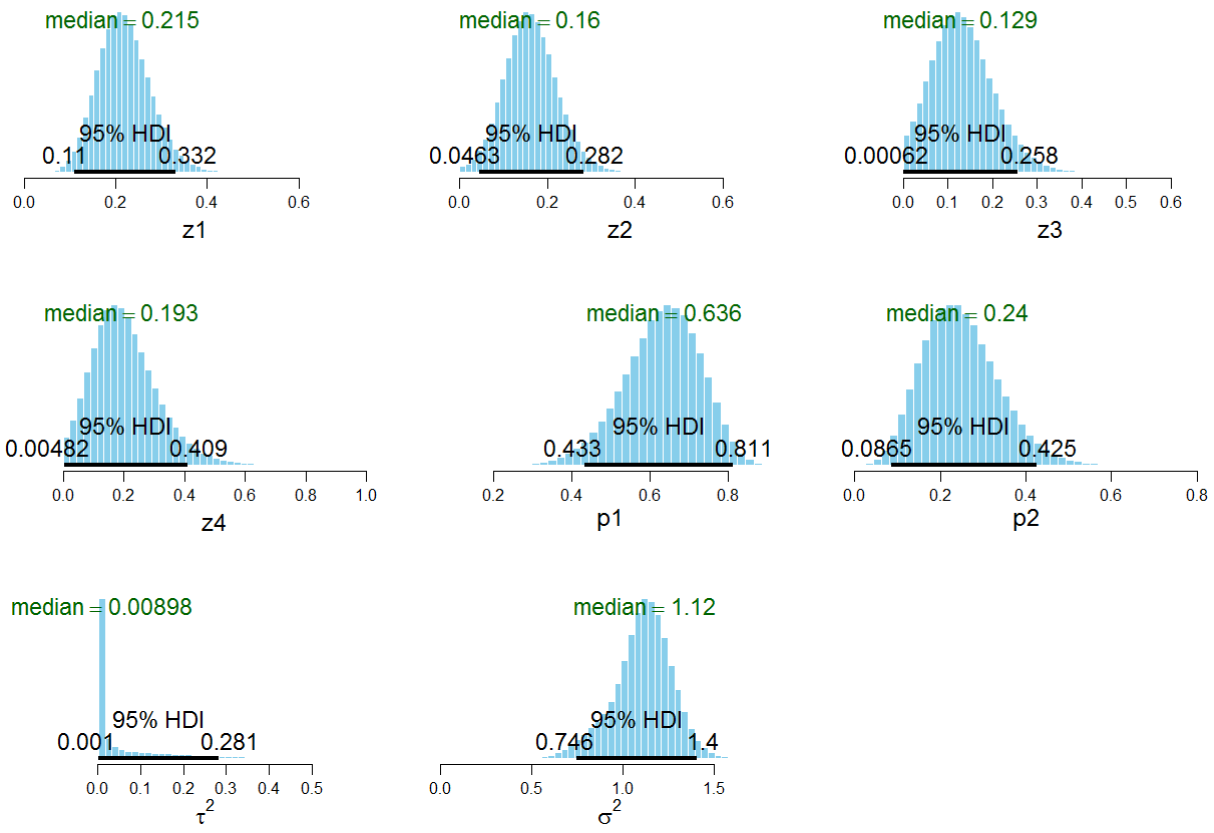


Figure B-1: Size-dependent survival (SDS) model parameter posterior distributions with median and 95% HDI.

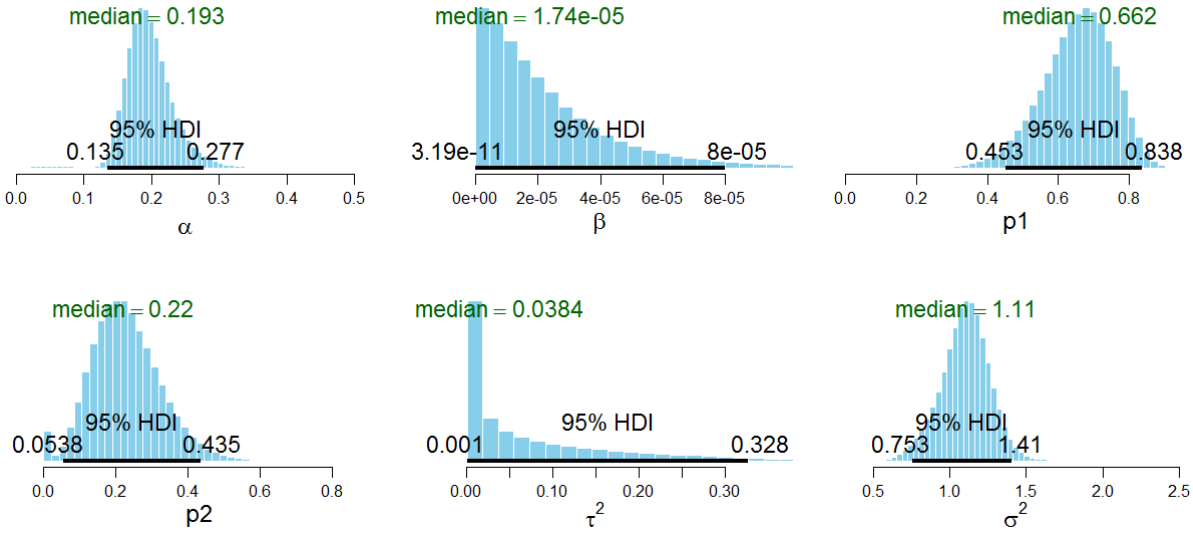


Figure B-2: Within stage density-dependent survival (BW) model parameter posterior distributions with median and 95% HDI.

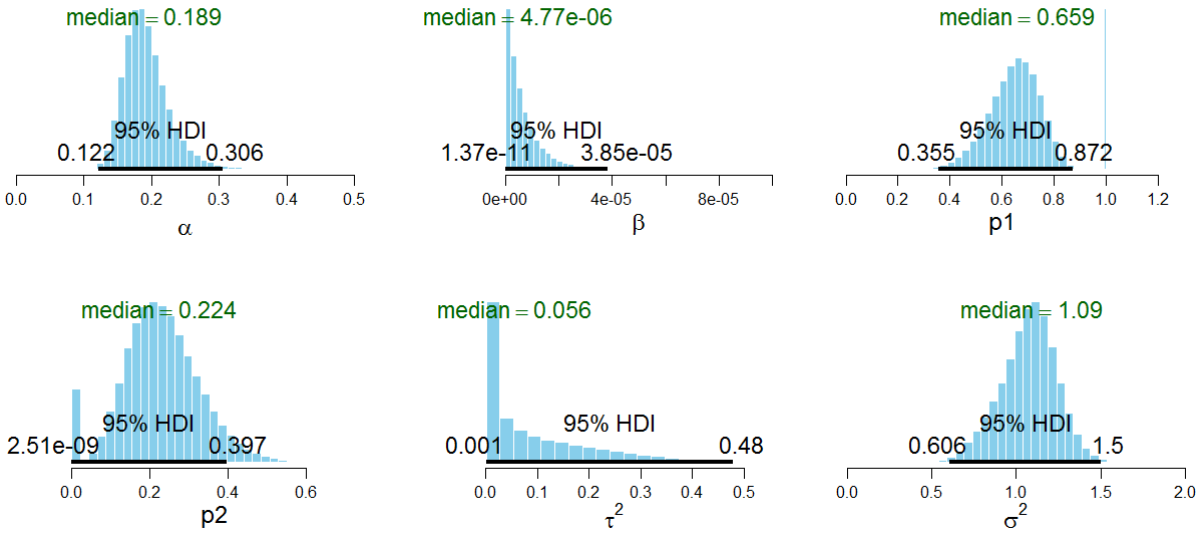


Figure B-3: Between all stage density-dependent survival (BA) model parameter posterior distributions with median and 95% HDI.

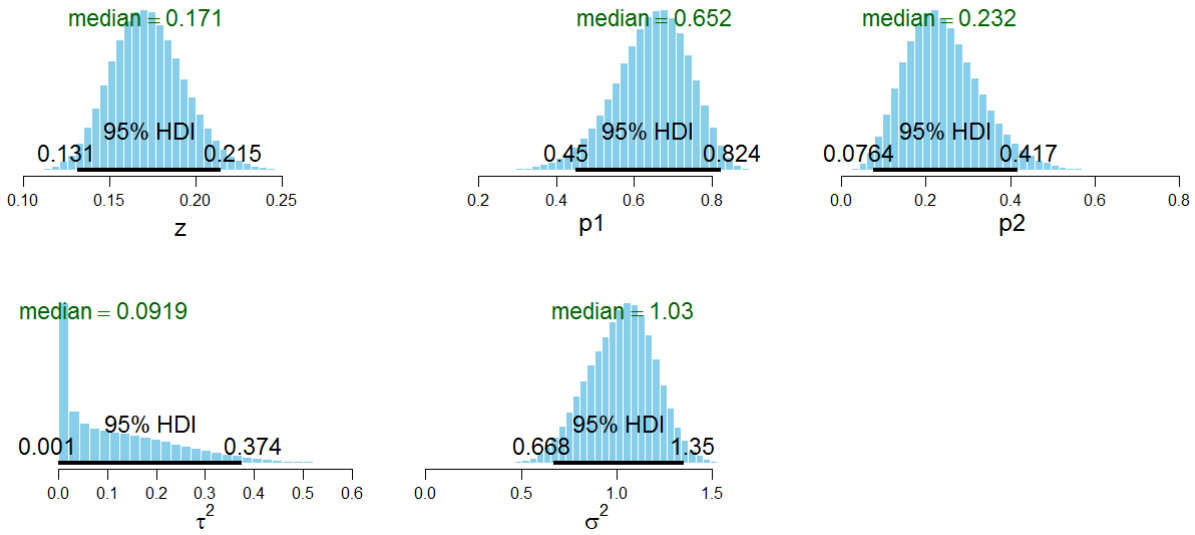


Figure B-4: Density and size-independent (NULL) model parameter posterior distributions with median and 95% HDI.

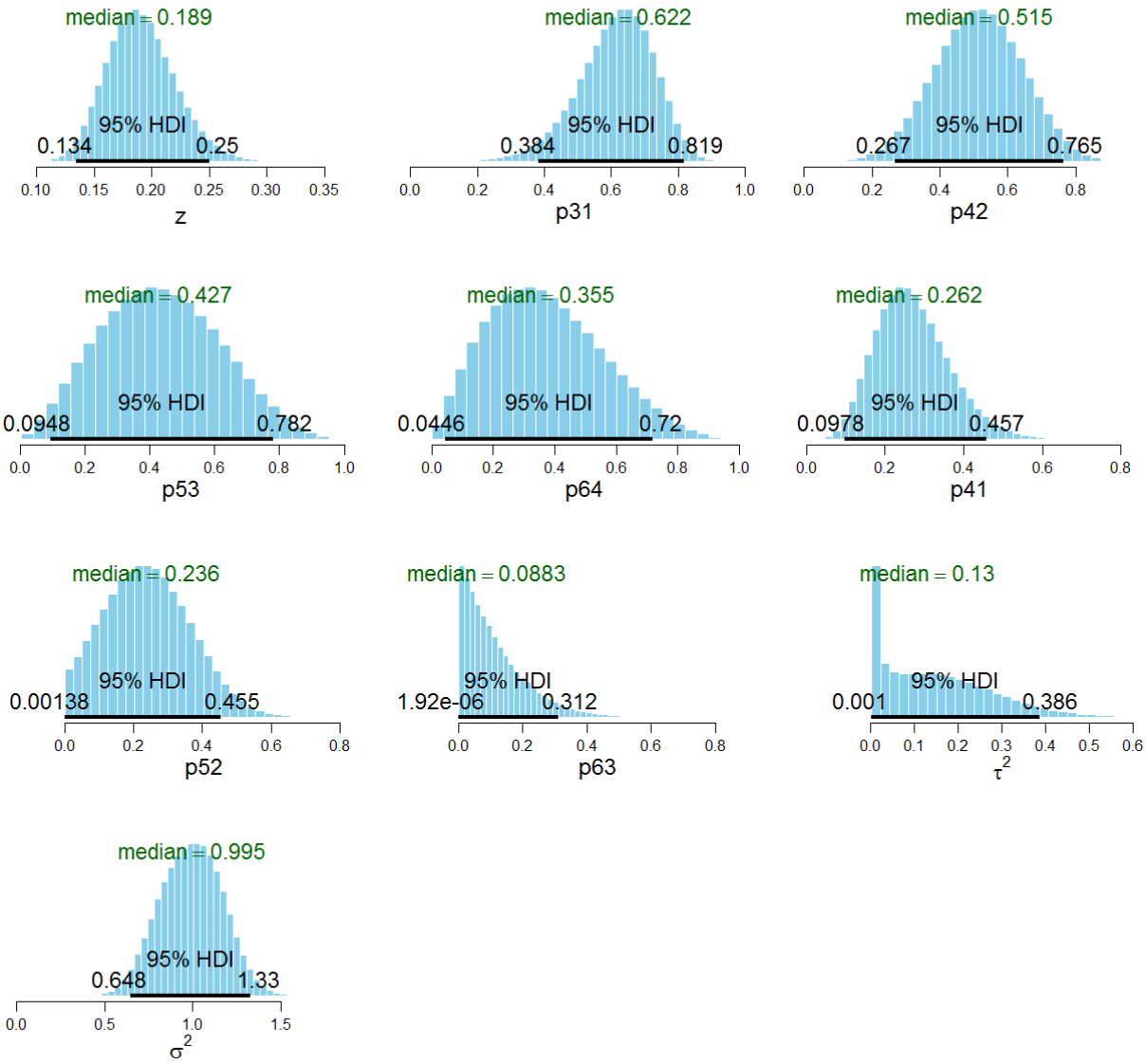


Figure B-5: Size-dependent growth (SDG) model parameter posterior distributions with median and 95% HDI.

# APPENDIX C

# ANNOTATED R CODE

**Size and Density-Independent Survival and Growth (NULL) Model**

```
library('runjags')                          #LOAD NECESSARY PACKAGES
library('rlecuyer')
str<-"
model {
for (i in 1:6)
{
  x[i,1] <- x0init*x0[i]                    #INITIAL POPULATION DENSITY
}
          for (i in 2:N)                    #MATRIX POPULATION MODEL (see section 2.4)
{
v[1,i]<-c11*s[1,i-1]+c12*s[2,i-1]+c13*s[3,i-1]+c14*s[4,i-1]
v[2,i]<-c21*s[1,i-1]+c22*s[2,i-1]+c23*s[3,i-1]+c24*s[4,i-1]
v[3,i]<-z*p1*x[1,i-1]+c31*s[1,i-1]+c32*s[2,i-1]+c33*s[3,i-1]+c34*s[4,i-1]
v[4,i]<-z*p2*x[1,i-1]+z*p1*x[2,i-1]
v[5,i]<-z*(1-p1-p2)*x[1,i-1]+z*p2*x[2,i-1]+z*p1*x[3,i-1]
v[6,i]<-z*(1-p1-p2)*x[2,i-1]+z*p2*x[3,i-1]+z*p1*x[4,i-1]

for (j in 1:6)
{
  x[j,i] ~ dlnorm(log(v[j,i]), 1/w.proc)    #TRUE POPULATION DENSITY (equation 2)
  y[j,i] ~ dlnorm(log(x[j,i]), 1/v.obs)     #OBSERVED POPULATION DENSITY (equation 1)
  }
}
                                            #PRIOR DISTRIBUTIONS (see section 2.6 for prior
                                            distributions descriptions and justification)
z~dunif(0,1)                                #SURVIVAL

a2[1]<-sum(alpha.a[2:3])                    #GROWTH
p1~dbeta(alpha.a[1],a2[1])

a2[2]<-alpha.a[3]
psi~dbeta(alpha.a[2],a2[1])
p2<-psi*(1-p1)

c11~dunif(0,10000)                          #SEASONAL SETTLEMENT
c12~dunif(0,10000)
c13~dunif(0,10000)
c14~dunif(0,10000)
c21~dunif(0,10000)
c22~dunif(0,10000)
c23~dunif(0,10000)
```

```
c24~dunif(0,10000)
c31~dunif(0,10000)
c32~dunif(0,10000)
c33~dunif(0,10000)
c34~dunif(0,10000)

v.obs ~ dunif(0.001, 10)              #OBSERVATION VARIANCE
w.proc ~ dunif(0.001, 10)             #PROCESS VARIANCE
x0init ~ dunif(1,10000)               #INITIAL POPULATION DENSITY
}
"
writeLines(str,con='p.ss.l.txt')
rm(str)
alpha.a=c(2,1,1)
y[y==0] <- NA

datalist=list(N=N, y=y, s=S, x0=c(y[1:3,1],1,1,1), alpha.a = alpha.a)

initx <- function(chain)              # INITIATE THE PARAMETERS
{
 set.seed(chain*13)
 err.inits = runif(2, 1e-3, 10)
 rec.inits = runif(12, 0, 1e4)
 psi.inits = rbeta(1,1,2)
 p1.inits = rbeta(1, alpha.a[1], sum(alpha.a[2:3]))
 z.inits = runif(2,0,1)

 rzl = list(
  w.proc = err.inits[1],
  v.obs = err.inits[2],
  z = z.inits[1],
  p1 = p1.inits[1],
  psi = psi.inits[1],
  c11 = rec.inits[1],
  c12 = rec.inits[2],
  c13 = rec.inits[3],
  c14 = rec.inits[4],
  c21 = rec.inits[5],
  c22 = rec.inits[6],
  c23 = rec.inits[7],
  c24 = rec.inits[8],
  c31 = rec.inits[9],
  c32 = rec.inits[10],
  c33 = rec.inits[11],
  c34 = rec.inits[12]
 )
 return(rzl)
}

#PARAMETERS TO MONITOR
parameters=c('z','p1','p2','c11','c12','c13','c14','c21','c22','c23','c24','c31','c32','c33','c34','v.obs','w.proc')
```

```
#SET TOTAL NUMBER OF CHAINS
chains = 7
load.module('lecuyer')
parallel.seeds('lecuyer::RngStream', chains)

#START SIMULATION
rzl<-run.jags(model='p.ss.l.txt', monitor=parameters, data=datalist, n.chains=chains, method='rjparallel',
inits=initx, summarise=TRUE, burnin=5e3, adapt=1e3, sample=1e3, thin=1e2)

#EXTEND SIMULATION UNTIL CONVERGED
rzl.l<-autoextend.jags(rzl, startsample=1e4, adapt=1e3, summarise = TRUE, interactive=FALSE,
max.time=Inf, jags.refresh = 30)

#CONVERT RESULTS TO CLASS(RUNJAGS)
rzl.l.jags<-as.jags(rzl.l, adapt=1000, quiet=FALSE)

#COMPUTE DIC AND pD
dic.l=dic.samples(rzl.l.jags, n.iter=10000, thin=1000, type='pD')
```

**Size-Dependent Survival (SDS) Model**

```
library('runjags')                    #LOAD NECESSARY PACKAGES
library('rlecuyer')
str<-"
model {
for (i in 1:6)
{
  x[i,1] <- x0init*x0[i]              #INITIAL POPULATION DENSITY
  y[i,1] ~ dlnorm(log(x[i,1]), 1/v.obs)
}
for (i in 2:N)                        #MATRIX POPULATION MODEL (see section 2.4)
{
v[1,i]<-c11*s[1,i-1]+c12*s[2,i-1]+c13*s[3,i-1]+c14*s[4,i-1]
v[2,i]<-c21*s[1,i-1]+c22*s[2,i-1]+c23*s[3,i-1]+c24*s[4,i-1]
v[3,i]<-z1*p1*x[1,i-1]+c31*s[1,i-1]+c32*s[2,i-1]+c33*s[3,i-1]+c34*s[4,i-1]
v[4,i]<-z1*p2*x[1,i-1]+z2*p1*x[2,i-1]
v[5,i]<-z1*(1-p1-p2)*x[1,i-1]+z2*p2*x[2,i-1]+z3*p1*x[3,i-1]
v[6,i]<-z2*(1-p1-p2)*x[2,i-1]+z3*p2*x[3,i-1]+z4*p1*x[4,i-1]
for (j in 1:6)
{
  x[j,i] ~ dlnorm(log(v[j,i]), 1/w.proc)   #TRUE POPULATION DENSITY (equation 2)
  y[j,i] ~ dlnorm(log(x[j,i]), 1/v.obs)    #OBSERVED POPULATION DENSITY (equation 1)
  }
}
                                      #PRIOR DISTRIBUTIONS (see section 2.6 for prior
                                      distributions descriptions and justification)
a2[1]<-sum(alpha[2:3])                #GROWTH
p1~dbeta(alpha[1],a2[1])

a2[2]<-alpha[3]
psi~dbeta(alpha[2],a2[1])
p2<-psi*(1-p1)

z1~dunif(0,1)                         #SURVIVAL
z2~dunif(0,1)
z3~dunif(0,1)
z4~dunif(0,1)

c11~dunif(0,10000)                    #SEASONAL SETTLEMENT
c12~dunif(0,10000)
c13~dunif(0,10000)
c14~dunif(0,10000)
c21~dunif(0,10000)
c22~dunif(0,10000)
c23~dunif(0,10000)
c24~dunif(0,10000)
c31~dunif(0,10000)
c32~dunif(0,10000)
c33~dunif(0,10000)
```

```
c34~dunif(0,10000)

v.obs ~ dunif(0.001, 10)                #OBSERVATION VARIANCE
w.proc ~ dunif(0.001, 10)               #PROCESS VARIANCE
x0init ~ dunif(1,10000)                 #INITIAL POPULATION DENSITY
}
"

writeLines(str,con='p.ss.sds.txt')
rm(str)
alpha = c(2,1,1)
y[y==0] <- NA

datalist=list(N=N, y=y, s=S, x0=c(y[1:3,1],1,1,1), alpha = alpha)

initx <- function(chain)                # INITIATE THE PARAMETERS

{
 set.seed(chain*13)
 err.inits = runif(2, 1e-3, 10)
 rec.inits = runif(12, 0, 1e4)
 psi.inits = rbeta(1,1,2)
 p1.inits = rbeta(1, alpha[1], sum(alpha[2:3]))
 z.inits = runif(4,0,1)

 rzl = list(
  w.proc = err.inits[1],
  v.obs = err.inits[2],
  z1 = z.inits[1],
  z2 = z.inits[2],
  z3 = z.inits[3],
  z4 = z.inits[4],
  p1 = p1.inits[1],
  psi = psi.inits[1],
  c11 = rec.inits[1],
  c12 = rec.inits[2],
  c13 = rec.inits[3],
  c14 = rec.inits[4],
  c21 = rec.inits[5],
  c22 = rec.inits[6],
  c23 = rec.inits[7],
  c24 = rec.inits[8],
  c31 = rec.inits[9],
  c32 = rec.inits[10],
  c33 = rec.inits[11],
  c34 = rec.inits[12]
 )
 return(rzl)
}
```

```
#PARAMETERS TO MONITOR
parameters=c('z1','z2','z3','z4','p1','p2','c11','c12','c13','c14','c21','c22','c23','c24','c31','c32','c33','c34','v.obs'
,'w.proc')

#SET TOTAL NUMBER OF CHAINS
chains = 7
load.module("lecuyer")
parallel.seeds('lecuyer::RngStream', chains)

#START SIMULATION
rzl<-run.jags(model='p.ss.sds.txt', monitor=parameters, data=datalist, n.chains=chains,
method='rjparallel', inits=initx, summarise=TRUE, burnin=5e3, adapt=1e3, sample=1e3, thin=1e2 )

#EXTEND SIMULATION UNTIL CONVERGED
rzl.sds<-autoextend.jags(rzl, startsample=1e4, adapt=1e3, summarise = TRUE, interactive=FALSE,
max.time=Inf, jags.refresh = 30)

#CONVERT RESULTS TO CLASS(RUNJAGS)
rzl.sds.jags<-as.jags(rzl.sds, adapt=1000, quiet=FALSE)

#COMPUTE DIC AND pD
dic.sds=dic.samples(rzl.sds.jags, n.iter=10000, thin=1000, type='pD')
```

**Size-dependent Growth (SDG) Model**

```
library('runjags')                    #LOAD NECESSARY PACKAGES
library('rlecuyer')

str<-"
model {
for (i in 1:6)
{
  x[i,1] <- x0init*x0[i]              #INITIAL POPULATION DENSITY
  y[i,1] ~ dlnorm(log(x[i,1]), 1/v.obs)
}
for (i in 2:N)                        #MATRIX POPULATION MODEL (see section 2.4)
{
v[1,i]<-c11*s[1,i-1]+c12*s[2,i-1]+c13*s[3,i-1]+c14*s[4,i-1]
v[2,i]<-c21*s[1,i-1]+c22*s[2,i-1]+c23*s[3,i-1]+c24*s[4,i-1]
v[3,i]<-z*p31*x[1,i-1]+c31*s[1,i-1]+c32*s[2,i-1]+c33*s[3,i-1]+c34*s[4,i-1]
v[4,i]<-z*p41*x[1,i-1]+z*p42*x[2,i-1]
v[5,i]<-z*(1-p31-p41)*x[1,i-1]+z*p52*x[2,i-1]+z*p53*x[3,i-1]
v[6,i]<-z*(1-p42-p52)*x[2,i-1]+z*p63*x[3,i-1]+z*p64*x[4,i-1]
for (j in 1:6)
  {
  x[j,i] ~ dlnorm(log(v[j,i]), 1/w.proc)   #TRUE POPULATION DENSITY (equation 2)
  y[j,i] ~ dlnorm(log(x[j,i]), 1/v.obs)    #OBSERVED POPULATION DENSITY (equation 1)
  }
}
                                      #PRIOR DISTRIBUTIONS (see section 2.6 for prior
                                      distributions descriptions and justification)
a2[1]<-sum(alpha[2:4])                #GROWTH
p31~dbeta(alpha[1],a2[1])
p42~dbeta(alpha[1],a2[1])
p53~dbeta(alpha[1],a2[1])
p64~dbeta(alpha[1],a2[1])

a2[2]<-sum(alpha[3:4])
psi2~dbeta(alpha[2],a2[2])
p41<-psi2*(1-sum(p31))
psi22~dbeta(alpha[2],a2[2])
p52<-psi22*(1-sum(p42))
psi32~dbeta(alpha[2],a2[2])
p63<-psi32*(1-sum(p53))

z~dunif(0,1)                          #SURVIVAL

c11~dunif(0,10000)                    #SEASONAL SETTLEMENT
c12~dunif(0,10000)
c13~dunif(0,10000)
c14~dunif(0,10000)
c21~dunif(0,10000)
c22~dunif(0,10000)
c23~dunif(0,10000)
```

```
c24~dunif(0,10000)
c31~dunif(0,10000)
c32~dunif(0,10000)
c33~dunif(0,10000)
c34~dunif(0,10000)

v.obs ~ dunif(0.001, 10)                #OBSERVATION VARIANCE
w.proc ~ dunif(0.001, 10)               #PROCESS VARIANCE
x0init ~ dunif(1,10000)                 #INITIAL POPULATION DENSITY
}
"
writeLines(str,con='p.ss.sdg.txt')
rm(str)
alpha=c(2,1,1,1)
y[y==0] <- NA

datalist=list(N=N, y=y, s=S, x0=c(y[1:3,1],1,1,1), alpha = alpha)

initx <- function(chain)                # INITIATE THE PARAMETERS
{
 set.seed(chain*13)
 err.inits = runif(2, 1e-3, 10)
 rec.inits = runif(12, 0, 1e4)
 psi.inits = rbeta(3,1,2)
 p.inits = rbeta(4, alpha[1], sum(alpha[2:3]))
 z.inits = runif(2,0,1)

 rzl = list(
  w.proc = err.inits[1],
  v.obs = err.inits[2],
  z = z.inits[1],
  p31 = p.inits[1],
  p42 = p.inits[2],
  p53 = p.inits[3],
  p64 = p.inits[4],
  psi2 = psi.inits[1],
  psi22 = psi.inits[2],
  psi32 = psi.inits[3],
  c11 = rec.inits[1],
  c12 = rec.inits[2],
  c13 = rec.inits[3],
  c14 = rec.inits[4],
  c21 = rec.inits[5],
  c22 = rec.inits[6],
  c23 = rec.inits[7],
  c24 = rec.inits[8],
  c31 = rec.inits[9],
  c32 = rec.inits[10],
  c33 = rec.inits[11],
  c34 = rec.inits[12]
 )
```

```
  return(rzl)
}

#PARAMETERS TO MONITOR
parameters=c('z','p31','p42','p53','p64','p41','p52','p63','c11','c12','c13','c14','c21','c22','c23','c24','c31','c32','
c33','c34','v.obs','w.proc')

#SET TOTAL NUMBER OF CHAINS
chains = 7
load.module('lecuyer')
parallel.seeds('lecuyer::RngStream', chains)

#START SIMULATION
rzl<-run.jags(model='p.ss.sdg.txt', monitor=parameters, data=datalist, n.chains=chains,
method='rjparallel', inits=initx, summarise=TRUE, burnin=5e3, adapt=1e3, sample=1e3, thin=1e2)

#EXTEND SIMULATION UNTIL CONVERGED
rzl.sdg<-autoextend.jags(rzl, startsample=1e4, adapt=1e3, summarise = TRUE, interactive=FALSE,
max.time=Inf, jags.refresh = 30)

#CONVERT RESULTS TO CLASS(RUNJAGS)
rzl.sdg.jags<-as.jags(rzl.sdg, adapt=1000, quiet=FALSE)

#COMPUTE DIC AND pD
dic.sdg=dic.samples(rzl.sdg.jags, n.iter=10000, thin=1000, type='pD')
```

**Within Stage Density-Dependent Survival (BW) Model**

```
library('runjags')                    #LOAD NECESSARY PACKAGES
library('rlecuyer')
str<-"
model {
for (i in 1:6)
{
 x[i,1] <- x0init*x0[i]               #INITIAL POPULATION DENSITY
y[i,1] ~ dlnorm(log(x[i,1]), 1/v.obs)
}
for (i in 2:N)                        #MATRIX POPULATION MODEL (see section 2.4)
{
v[1,i]<-c11*s[1,i-1]+c12*s[2,i-1]+c13*s[3,i-1]+c14*s[4,i-1]
v[2,i]<-c21*s[1,i-1]+c22*s[2,i-1]+c23*s[3,i-1]+c24*s[4,i-1]
v[3,i]<-((alpha)/(1+(beta*x[1,i-1])))*p1*x[1,i-1]+c31*s[1,i-1]+c32*s[2,i-1]+c33*s[3,i-1]+c34*s[4,i-1]
v[4,i]<-((alpha)/(1+(beta*x[1,i-1])))*p2*x[1,i-1]+((alpha)/(1+(beta*x[2,i-1])))*p1*x[2,i-1]
v[5,i]<-((alpha)/(1+(beta*x[1,i-1])))*(1-p1-p2)*x[1,i-1]+((alpha)/(1+(beta*x[2,i-1])))*p2*x[2,i-
1]+((alpha)/(1+(beta*x[3,i-1])))*p1*x[3,i-1]
v[6,i]<-((alpha)/(1+(beta*x[2,i-1])))*(1-p1-p2)*x[2,i-1]+((alpha)/(1+(beta*x[3,i-1])))*p2*x[3,i-
1]+((alpha)/(1+(beta*x[4,i-1])))*p1*x[4,i-1]
for (j in 1:6)
{
x[j,i] ~ dlnorm(log(v[j,i]), 1/w.proc)   #TRUE POPULATION DENSITY (equation 2)
y[j,i] ~ dlnorm(log(x[j,i]), 1/v.obs)    #OBSERVED POPULATION DENSITY (equation 1)
}
}
                                      #PRIOR DISTRIBUTIONS (see section 2.6 for prior
                                      distributions descriptions and justification)
a2[1]<-sum(alpha.a[2:3])              #GROWTH
p1~dbeta(alpha.a[1],a2[1])

a2[2]<-alpha.a[3]
psi~dbeta(alpha.a[2],a2[1])
p2<-psi*(1-p1)

alpha~dunif(0,1)                      #BEVERTON-HOLT DENSITY-DEPENDENT SURVIVAL
beta~dunif(0,1e7)


c11~dunif(0,10000)                    #SEASONAL SETTLEMENT
c12~dunif(0,10000)
c13~dunif(0,10000)
c14~dunif(0,10000)
c21~dunif(0,10000)
c22~dunif(0,10000)
c23~dunif(0,10000)
c24~dunif(0,10000)
c31~dunif(0,10000)
c32~dunif(0,10000)
c33~dunif(0,10000)
```

```
c34~dunif(0,10000)

v.obs ~ dunif(0.001, 10)                #OBSERVATION VARIANCE
w.proc ~ dunif(0.001, 10)               #PROCESS VARIANCE
x0init ~ dunif(1,10000)                 #INITIAL POPULATION DENSITY
}
"
writeLines(str,con='p.ss.wdds.txt')
rm(str)
alpha.a=c(2,1,1)
y[y==0] <- NA

datalist=list(N=N, y=y, s=S, x0=c(y[1:3,1],1,1,1), alpha.a = alpha.a)

initx <- function(chain)                # INITIATE THE PARAMETERS
{
  set.seed(chain*13)
  err.inits = runif(2, 1e-3, 10)
  rec.inits = runif(12, 0, 1e4)
  psi.inits = rbeta(1,1,2)
  p1.inits = rbeta(1, alpha.a[1], sum(alpha.a[2:3]))
  alpha.inits = runif(1,0,1)
  beta.inits = runif(1,0,1e7)

  rzl = list(
    w.proc = err.inits[1],
    v.obs = err.inits[2],
    alpha = alpha.inits[1],
    beta = beta.inits[1],
    p1 = p1.inits[1],
    psi = psi.inits[1],
    c11 = rec.inits[1],
    c12 = rec.inits[2],
    c13 = rec.inits[3],
    c14 = rec.inits[4],
    c21 = rec.inits[5],
    c22 = rec.inits[6],
    c23 = rec.inits[7],
    c24 = rec.inits[8],
    c31 = rec.inits[9],
    c32 = rec.inits[10],
    c33 = rec.inits[11],
    c34 = rec.inits[12]
  )
  return(rzl)
}

#PARAMETERS TO MONITOR
parameters=c('alpha','beta','p1','p2','c11','c12','c13','c14','c21','c22','c23','c24','c31','c32','c33','c34','v.obs','w
.proc')
```

```
#SET TOTAL NUMBER OF CHAINS
chains = 7
load.module('lecuyer')
parallel.seeds('lecuyer::RngStream', chains)

#START SIMULATION
rzl<-run.jags(model='p.ss.wdds.txt', monitor=parameters, data=datalist, n.chains=chains,
method='rjparallel', inits=initx, summarise=TRUE, burnin=5e3, adapt=1e3, sample=1e3, thin=1e2)

#EXTEND SIMULATION UNTIL CONVERGED
rzl.wdds<-autoextend.jags(rzl, startsample=1e4, adapt=1e3, summarise = TRUE, interactive=FALSE,
max.time=Inf, jags.refresh = 30)

#CONVERT RESULTS TO CLASS(RUNJAGS)
rzl.wdds.jags<-as.jags(rzl.wdds, adapt=10000, quiet=FALSE)

#COMPUTE DIC AND pD
dic.wdds=dic.samples(rzl.wdds.jags, n.iter=100000, thin=1000, type='pD' )
```

**Between All Stages Density-Dependent Survival (BA) Model**

```
library('runjags')                          #LOAD NECESSARY PACKAGES
library('rlecuyer')
str<-"
model {
for (i in 1:6)
{
  x[i,1] <- x0init*x0[i]                    #INITIAL POPULATION DENSITY
  y[i,1] ~ dlnorm(log(x[i,1]), 1/v.obs)
}
for (i in 2:N)                              #MATRIX POPULATION MODEL (see section 2.4)
{
v[1,i]<-c11*s[1,i-1]+c12*s[2,i-1]+c13*s[3,i-1]+c14*s[4,i-1]
v[2,i]<-c21*s[1,i-1]+c22*s[2,i-1]+c23*s[3,i-1]+c24*s[4,i-1]
v[3,i]<-(alpha)/(1+beta*(sum(x[1:6,i-1])))*p1*x[1,i-1]+c31*s[1,i-1]+c32*s[2,i-1]+c33*s[3,i-
1]+c34*s[4,i-1]
v[4,i]<-(alpha)/(1+beta*(sum(x[1:6,i-1])))*p2*x[1,i-1]+(alpha)/(1+beta*(sum(x[1:6,i-1])))*p1*x[2,i-1]
v[5,i]<-(alpha)/(1+beta*(sum(x[1:6,i-1])))*(1-p1-p2)*x[1,i-1]+(alpha)/(1+beta*(sum(x[1:6,i-
1])))*p2*x[2,i-1]+(alpha)/(1+beta*(sum(x[1:6,i-1])))*p1*x[3,i-1]
v[6,i]<-(alpha)/(1+beta*(sum(x[1:6,i-1])))*(1-p1-p2)*x[2,i-1]+(alpha)/(1+beta*(sum(x[1:6,i-
1])))*p2*x[3,i-1]+(alpha)/(1+beta*(sum(x[1:6,i-1])))*p1*x[4,i-1]
for (j in 1:6)
  {
  x[j,i] ~ dlnorm(log(v[j,i]), 1/w.proc)    #TRUE POPULATION DENSITY (equation 2)
  y[j,i] ~ dlnorm(log(x[j,i]), 1/v.obs)     #OBSERVED POPULATION DENSITY (equation 1)
  }
}
                                            #PRIOR DISTRIBUTIONS (see section 2.6 for prior
                                            distributions descriptions and justification)
a2[1]<-sum(alpha.a[2:3])                    #GROWTH
p1~dbeta(alpha.a[1],a2[1])

a2[2]<-alpha.a[3]
psi~dbeta(alpha.a[2],a2[1])
p2<-psi*(1-p1)

alpha~dunif(0,1)                            #BEVERTON-HOLT DENSITY-DEPENDENT SURVIVAL
beta~dunif(0,1e7)


c11~dunif(0,10000)                          #SEASONAL SETTLEMENT
c12~dunif(0,10000)
c13~dunif(0,10000)
c14~dunif(0,10000)
c21~dunif(0,10000)
c22~dunif(0,10000)
c23~dunif(0,10000)
c24~dunif(0,10000)
c31~dunif(0,10000)
```

```
c32~dunif(0,10000)
c33~dunif(0,10000)
c34~dunif(0,10000)

v.obs ~ dunif(0.001, 10)                #OBSERVATION VARIANCE
w.proc ~ dunif(0.001, 10)               #PROCESS VARIANCE
x0init ~ dunif(1,10000)                 #INITIAL POPULATION DENSITY
}
"
writeLines(str,con='p.ss.btdds.txt')
rm(str)
alpha.a=c(2,1,1)
y[y==0] <- NA

datalist=list(N=N, y=y, s=S, x0=c(y[1:3,1],1,1,1), alpha.a = alpha.a)

initx <- function(chain)                #INITIATE THE PARAMETERS

{

 set.seed(chain*13)

 err.inits = runif(2, 1e-3, 10)

 rec.inits = runif(12, 0, 1e4)

 psi.inits = rbeta(1,1,2)

 p1.inits = rbeta(1, alpha.a[1], sum(alpha.a[2:3]))

 alpha.inits = runif(1,0,1)

 beta.inits = runif(1,0,1e7)



 rzl = list(

  w.proc = err.inits[1],

  v.obs = err.inits[2],

  alpha = alpha.inits[1],

  beta = beta.inits[1],

  p1 = p1.inits[1],
```

```
    psi = psi.inits[1],

    c11 = rec.inits[1],

    c12 = rec.inits[2],

    c13 = rec.inits[3],

    c14 = rec.inits[4],

    c21 = rec.inits[5],

    c22 = rec.inits[6],

    c23 = rec.inits[7],

    c24 = rec.inits[8],

    c31 = rec.inits[9],

    c32 = rec.inits[10],

    c33 = rec.inits[11],

    c34 = rec.inits[12]

  )

  return(rzl)

}


#PARAMETERS TO MONITOR
parameters=c('alpha','beta','p1','p2','c11','c12','c13','c14','c21','c22','c23','c24','c31','c32','c33','c34','v.obs','w
.proc')

#SET TOTAL NUMBER OF CHAINS
chains = 3
load.module('lecuyer')
parallel.seeds('lecuyer::RngStream', chains)

#START SIMULATION
rzl<-run.jags(model='p.ss.btdds.txt', monitor=parameters, data=datalist, n.chains=chains,
method='rjparallel', inits=initx, summarise=TRUE, burnin=5e3, adapt=1e3, sample=1e3, thin=1e2)

#EXTEND SIMULATION UNTIL CONVERGED
```

```
rzl.btdds<-autoextend.jags(rzl.btdds, startsample=1e4, adapt=1e3, summarise = TRUE,
interactive=FALSE, max.time=Inf, jags.refresh = 30)

#CONVERT RESULTS TO CLASS(RUNJAGS)
rzl.btdds.jags<-as.jags(rzl.btdds, adapt=1000, quiet=FALSE)

#COMPUTE DIC AND pD
dic.btdds=dic.samples(rzl.btdds.jags, n.iter=10000, thin=1000, type='pD')
```